SAND76-8022
Unlimited Release

UC-62

Eye Hazard and Glint Evaluation for the 5-MW_t Solar Thermal Test Facility

T. D. Brumleve

Prepared by Sandia Laboratories, Albuquerque, New Mexico 87115 and Livermore, California 94550 for the United States Energy Research and Development Administration under Contract AT (29-1)-789

Printed May 1977

Sandia Laboratories
energy report

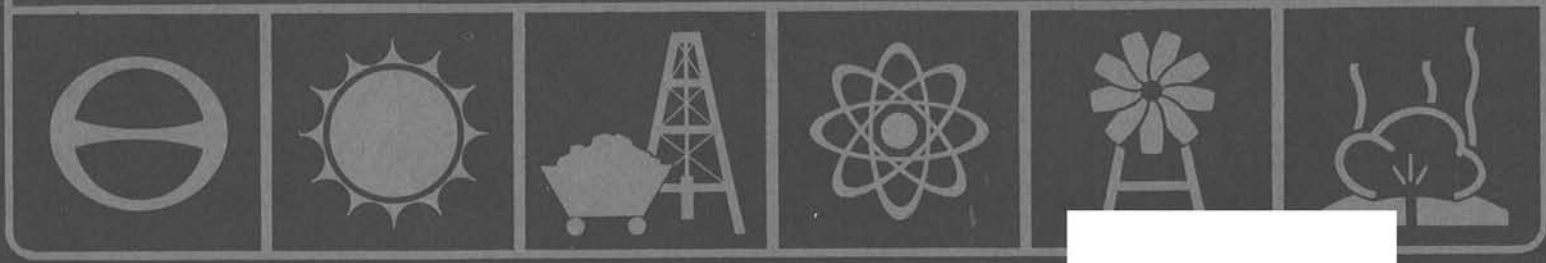

2900-QQB(3-74)

Issued by Sandia Laboratories, operated for the United States Energy Research & Development Administration by Sandia Corporation.

SF 1004-DF (3-75)

Printed in the United States of America
Available from
National Technical Information Service
U. S. Department of Commerce
5285 Port Royal Road
Springfield, VA 22161
Price: Printed Copy $4.50; Microfiche $3.00

UC-62

SAND76-8022
Unlimited Release
Printed May 1977

EYE HAZARD AND GLINT EVALUATION FOR THE 5-MW_t SOLAR THERMAL TEST FACILITY

T. D. Brumleve
Solar Energy Technology Division 8184
Sandia Laboratories

ABSTRACT

Potential eye hazards associated with concentrated reflected light are evaluated for the ERDA 5-MW_t Solar Thermal Test Facility to be constructed at Sandia Laboratories, Albuquerque, New Mexico. Light intensities and hazardous ranges of single and multiple coincident heliostat beams are evaluated at ground level and in the air space above the facility. Possible long-range and short-range effects of distractive effects of reflected beams are discussed. Also described are certain beam control modifications which were incorporated to minimize the altitudes at which overflying aircraft could encounter unsafe levels. Recommendations are made for further evaluation of intensity excursions during fail-safe shutdown situations, and for experiments to verify analytical models and to assess distractive glint effects.

TABLE OF CONTENTS

	Page
Introduction	9
Reflected Beam Intensities	12
Single Heliostat Beam	12
Multiple Coincident Beams	18
Eye Hazard Thresholds	19
Retinal Burns	19
Distractive Glint	32
Control Measures	33
Exclusion Zones	34
Beam Control Techniques	36
Other Potential Hazards	52
Fail-Safe Shutdown	52
Reflected Light From Receivers	52
Skin Burn	54
Fire Hazards	55
Suggested Experiments	55
Conclusions and Recommendations	56
Appendix A--References	59

ILLUSTRATIONS

Figure		Page
1.	Solar Test Facility	10
2.	Test Facility Plot Plan	11
3.	Heliostat Beam Geometry	12
4.	Beam Intensity Versus Distance	16
5.	Distance at Which Single Beam Intensity Rises Above One Sun Versus Focal Length	16
6.	Distance at Which Single Beam Intensity Drops Below One Sun Versus Focal Length	17
7.	Heliostat Array Focusing Geometry	18
8.	Number of Coincident Beams Required to Produce One-Sun Intensity	20
9.	Distance at Which an Intensity of One Sun Could be Produced by a Given Number of Coincident Beams	20
10.	Typical Light Sources and Eye Damage Thresholds	22
11.	Geometry of the Human Eye	23
12.	Single Beam Retinal Irradiance Relative to Safe Levels as a Function of Distance and Focal Length	27
13.	Number of Adjacent Beams Corresponding to Safe Retinal Irradiance as a Function of Distance, Focal Length and Projected Area Density	29
14.	Reflectance of the Atmosphere-Water Interface as a Function of the Angle of Incidence for External and Internal Reflections	33
15.	Flux Density of Five Coincident Beams Versus Distance	34
16.	Hemispherical Exclusion Zones Based on One Sun Intensity for Multiple Coincident Beams	35
17.	Hemispherical Exclusion Zones Based on Maximum Permissible Retinal Exposure for Multiple Coalesced Beams	35

Figure		Page
18.	Altitude at Which a One-Sun Intensity Could be Produced by a Given Number of Coincident Beams With Elevation Angle Limitation	39
19.	Number of Coincident Beams Corresponding to Safe Retinal Irradiance as a Function of Altitude, Focal Length and Projected Area Density With Elevation Angle Limitation	40
20.	Altitude at Which Retinal Exposure Drops to a Safe Level as a Function of Number of Coincident Beams With Elevation Angle Limitation	40
21.	Beam Disengagement Geometry With Zero Tracking Error	41
22.	Altitude at Which Two Adjacent Beams of a Given Separation and Focal Length Disengage With Elevation Angle Limitation and Zero Tracking Error	43
23.	Beam Disengagement Geometry Considering Tracking Errors	43
24.	Altitude at Which Two Adjacent Beams of a Given Separation and Focal Length Disengage With Angle Limitation and ±10 Milliradian Tracking Error	46
25.	Normal Projection of Beams Surrounding a Reference Heliostat 195 m North of the Tower	47
26.	Cumulative Number of Beams as a Function of Center-to-Center Distance From a Heliostat Beam 195 m North of Tower	48
27.	Progressive Expansion and Divergence of a Cluster of Ten Beams Centered 195 m North of Tower as a Function of Altitude	49
28.	Normal Projection of Beams Surrounding a Reference Heliostat 70 m North of Tower	50
29.	Recommended Aircraft Exclusion Zone Based on Safe Retinal Exposure to Reflected Light	51
30.	Pig Skin Injury Data	54

EYE HAZARD AND GLINT EVALUATION FOR THE 5-MW_t SOLAR THERMAL TEST FACILITY

Introduction

One important safety consideration for the 5-MW_t Solar Thermal Test Facility (STTF) under construction at Sandia Laboratories, Albuquerque, New Mexico is the potential eye hazard and distractive effect of sunlight reflected from the heliostats. As currently planned, this facility will consist of a centrally located 60-meter high tower with about 315 heliostats, as shown in Figures 1 and 2.* The heliostats will be movable and will be deployed either in a 360-degree configuration (Zones A, C, D, and E) or exclusively in the north field (Zones A and B).** Each heliostat will be approximately square, with 37 square meters of reflective surface made up of 25 individual, slightly dished mirrors (or facets). Each facet is focused and aimed so that the reflected light is concentrated at the receiver at the top of the tower.

In addition to the obvious safety hazards posed by the intense light near the focal zone, consideration must be given to the safety of persons at ground level and to potential hazards to aircraft resulting from single or multiple coincident beams directed into the airspace above the test facility. Maximum safe exposure levels for high intensity light are normally set by damage to the retina of the human eye. The intensity threshold above which permanent damage may occur depends on the spectrum, source angle, and duration of the light exposure. The natural aversion to bright light and involuntary blink reflexes also serve to limit retinal exposure time. Later

*A detailed description is contained in References 1, 2, and 3.

**An initial 1-MW_t capability will be provided by about 78 heliostats in Zone A supplied by Martin Marietta.

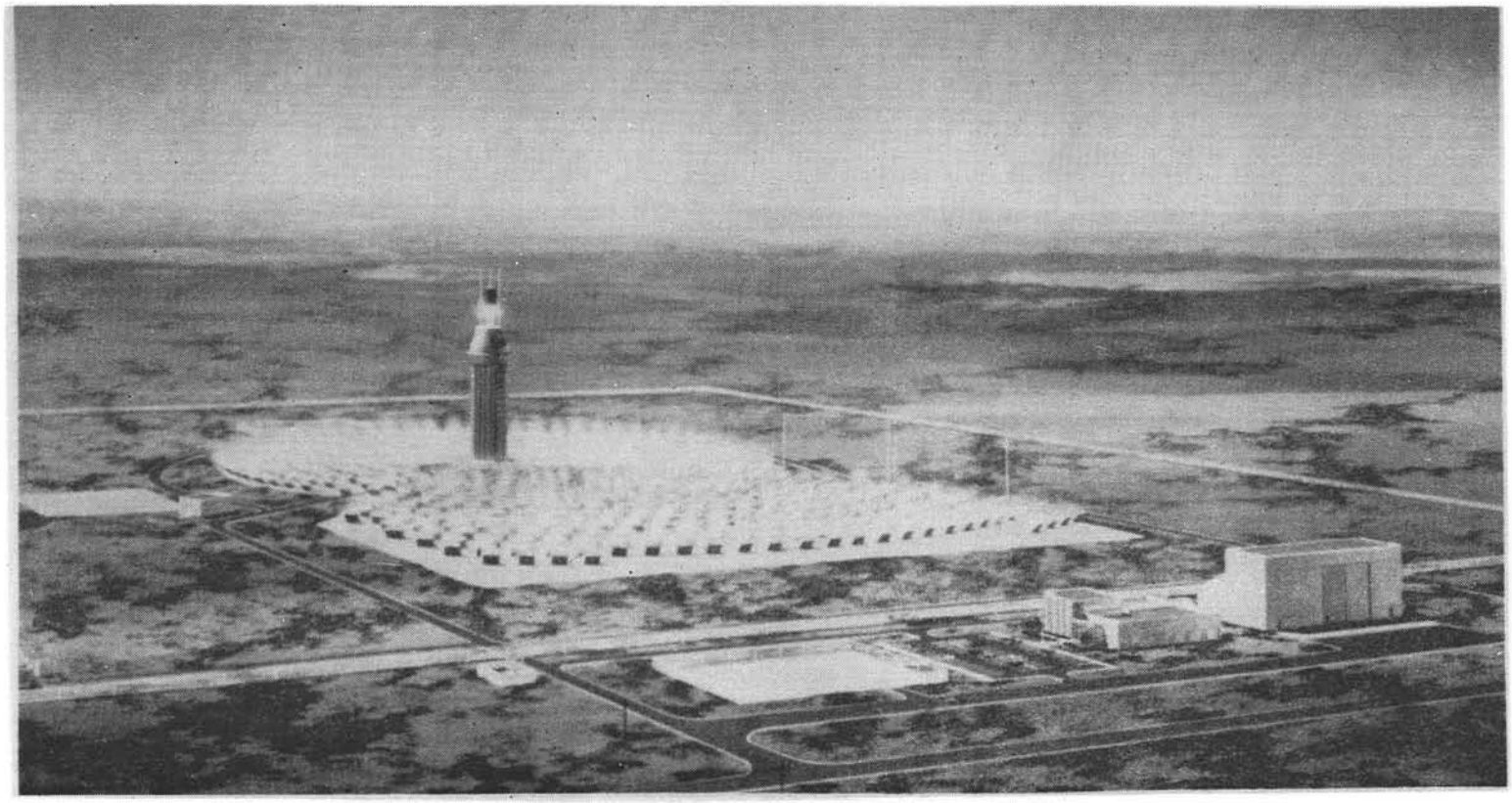

Figure 1. Solar Test Facility

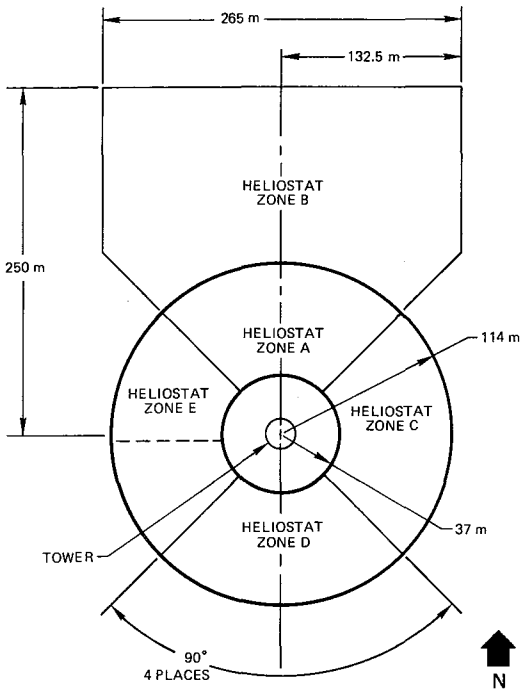

Figure 2. Test Facility Plot Plan

in this report a reflected intensity of one sun* is shown to be a conservative safe limit for momentary eye exposures for the several STTF configurations investigated.

In addition to these direct eye hazards, certain secondary effects must also be considered. Light intensities considerably below one sun can be distracting and can induce momentary flash blindness. There might, for example, be situations in which an unexpected flash could cause an aircraft or automobile accident. The possible importance of such effects is difficult to judge because in addition to intensity, such factors as (a) whether a flash is expected or comes as a complete surprise, (b) the criticalness of maneuvers at that instant, and (c) individual reactions are involved.

In the succeeding sections, expressions are first developed to characterize the flux density versus distance for an individual heliostat beam. The analysis is then extended to determine the number of coincident beams required at various distances to produce a given beam intensity. These relationships are then used to evaluate retinal hazards and to consider possible distractive effects. Various methods are discussed for controlling the

*Flux intensity equivalent to maximum direct normal insolation at ground level.

heliostats during normal operations or fail-safe shutdown so as to reduce the altitude at which overflying aircraft might encounter unsafe levels of concentrated light. The particular method which was incorporated is then evaluated. The potential intensity of light reflected from diffuse or specular surfaces of receivers or other items near the top of the tower is also evaluated with respect to the safety of personnel within the heliostat field, in facility buildings, or in other ground level locations. Finally, conclusions are presented and recommendations are made for further investigation of certain operational situations and for experiments to verify analytical models and to assess distractive effects.

Reflected Beam Intensities

Single Heliostat Beam

The focusing/defocusing geometry for a single heliostat beam is shown in Figure 3. This geometry is based upon the following assumptions:

1. Uniform sun intensity (no limb darkening)
2. Round, focused, continuous surface heliostats
3. No cosine losses or off-axis aberrations
4. Uniform intensity in beam cross section

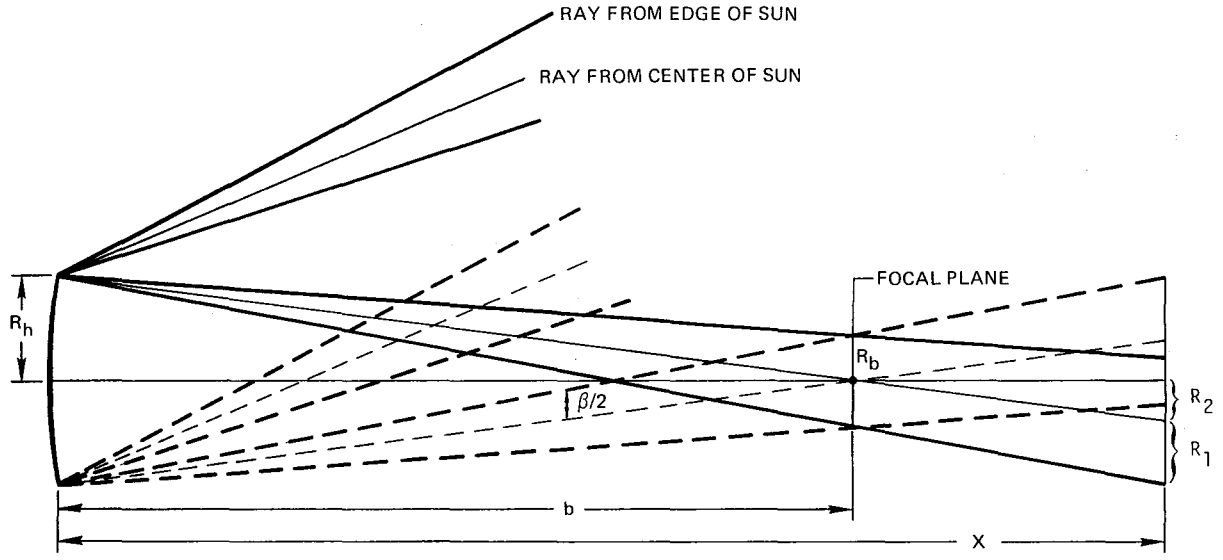

Figure 3. Heliostat Beam Geometry

The radius R_x of the beam cross section at a distance x can be considered to have two components:

$$R_x = R_1 + R_2$$

R_1 represents that portion of the total beam divergence due to sun angle and mirror contour inaccuracies. R_1 is expressed as

$$R_1 \approx x \tan \beta/2 *$$

where $\beta/2$ is the half angle of the total beam divergence. R_2 is the component of R_x due to the focusing/defocusing characteristic of the beam short of, or beyond, its focal length. R_2 is expressed as

$$R_2 = \frac{|x - b|}{b} R_h = \left|\frac{x}{b} - 1\right| R_h$$

where b is the heliostat focal length and R_h is the heliostat radius. Combining R_1 and R_2 yields

$$R_x = x \tan \beta/2 + \left|\frac{x}{b} - 1\right| R_h$$

When $\beta/2$ is small,

$$R_x \approx \frac{x\beta}{2} + \left|\frac{x}{b} - 1\right| R_h \qquad (1)$$

The geometric concentration C of the beam at the distance x is the ratio of the heliostat area A_h to the area of the beam cross section A_x. Thus,

$$C = \frac{A_h}{A_x} = \left(\frac{R_h}{R_x}\right)^2 = \left(\frac{R_h}{\frac{x\beta}{2} + \left|\frac{x}{b} - 1\right| R_h}\right)^2$$

*An approximation for relatively long focal length mirrors (error is less than 0.3% for $b/R_h > 18$).

Dividing by R_h and substituting $D_h = 2R_h$,

$$C = \left(\frac{1}{\frac{x\beta}{D_h} + \left| \frac{x}{b} - 1 \right|} \right)^2$$

The flux density or intensity I in "suns" is

$$I = \frac{F}{Q} = \rho C = \rho \left(\frac{1}{\frac{x\beta}{D_h} + \left| \frac{x}{b} - 1 \right|} \right)^2 \qquad (2)$$

where F is the flux density (power per unit area), Q is the direct normal insolation, and ρ is the specular reflectivity of the heliostat.

All of the parameters in Equation (2) are now known or can be reasonably estimated for the initial test facility heliostats. Assuming a focused, round heliostat with an area equal to that of the test facility heliostats, *

$$A_h = 37 \text{ m}^2$$

$$D_h = \left(\frac{4 A_h}{\pi} \right)^{0.5} = 6.86 \text{ m}$$

The beam quality specification for the test facility requires that at least 90% of the reflected energy be within a 0.012 radian total divergence angle.[3] Making the conservative assumption that all of the reflected energy falls within this angle,

$$\beta = 0.012 \text{ radian}$$

*Each of the heliostats being initially procured for Zone A is made up of 25 four-foot square focused facets arranged in a 5 x 5 square matrix. However, with the conservative assumptions of no cosine losses and no off-axis aberrations, the simplifying assumption of an equal area round mirror is believed to be justified. On either side of the focal zone the beam shape would be somewhat different from that from a square mirror, but the average beam intensity would be essentially the same.

The mirror reflectivity ρ is expected to be between 0.8 and 0.9 when the mirrors are new and clean. In this study, $\rho = 0.9$ is assumed. The focal lengths of the heliostats will vary according to their slant range to the receiver under test. Minimum, mean, and maximum slant ranges for the principal test zones are shown in Table I.

TABLE I

HELIOSTAT FOCAL LENGTHS

Zone	Receiver Height (m)	Number of Heliostats	Ground Radius (m)			Focal Length (m)		
			min	mean	max	min	mean	max
A	44	78	37	83	114	58	100	122
A, B	60	294	37	188	283	71	200	289
A, C, D, E	70	312	37	83	114	79	108	134

The beam intensities for the focal lengths of interest are shown versus distance in Figure 4. Note how the beam intensity at the focal plane decreases as the focal length increases. Also, the beam intensity of a focused heliostat at twice its focal length is equal to that of a flat heliostat at the same distance. Beyond twice its focal length, the beam intensity of a focused heliostat drops more rapidly than that of a flat heliostat, with the shorter focal lengths having the greatest rates of decrease.

The distance from the heliostat at which the beam intensity rises above one sun (x_1') can be derived from Equation (2):*

$$x_1' = \frac{1 - \rho^{0.5}}{\frac{1}{b} - \frac{\beta}{D_h}} \qquad (x \leqq b) \qquad (3)$$

This distance varies from about 3.8 meters for a 66-meter focal length heliostat to 32 meters for one with a 300-meter focal length (Figure 5). The distance from the heliostat at which the beam intensity drops to a level of one sun (x_1) is

*The one sun intensity introduced here as a reference threshold is discussed later under "Eye Hazard Thresholds." This is shown to be conservative based on retinal exposures for the source angles involved.

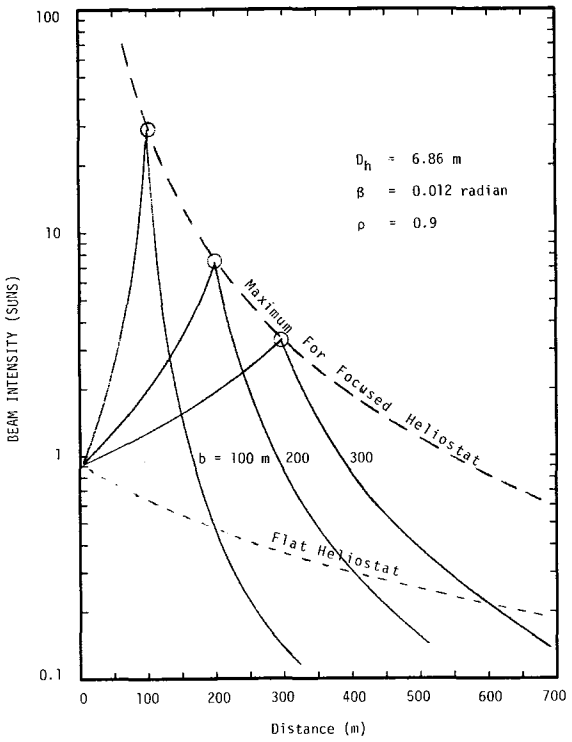

Figure 4. Beam Intensity Versus Distance

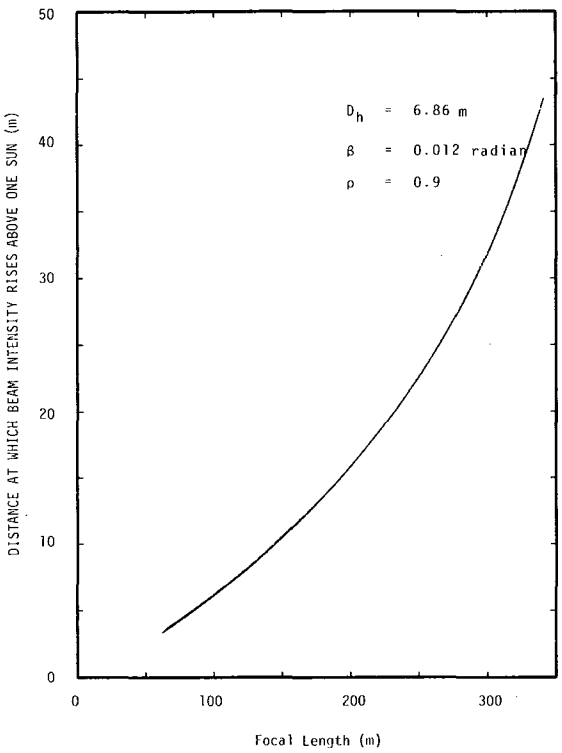

Figure 5. Distance at Which Single Beam Intensity Rises Above One Sun Versus Focal Length

$$x_1 = \frac{1 + \rho^{0.5}}{\frac{1}{b} + \frac{\beta}{D_h}} \qquad (x \geq b) \qquad (4)$$

This "one sun" distance is shown versus focal length in Figure 6. As is evident in both Figure 4 and Figure 6, the heliostat which can produce a one-sun intensity at the greatest distance is the heliostat with the greatest focal length. For the test facility, the maximum focal length would be about 289 meters, and the maximum distance at which this heliostat could produce a one-sun intensity would be about 375 meters. Thus, aircraft at altitudes higher than 375 meters above the facility or farther than 375 meters from its perimeter could never be exposed to more than one-sun intensity from any single heliostat beam. The one-sun distance for a 200-meter focal length heliostat (the appropriate mean for Zones A and B) is about 290 meters.

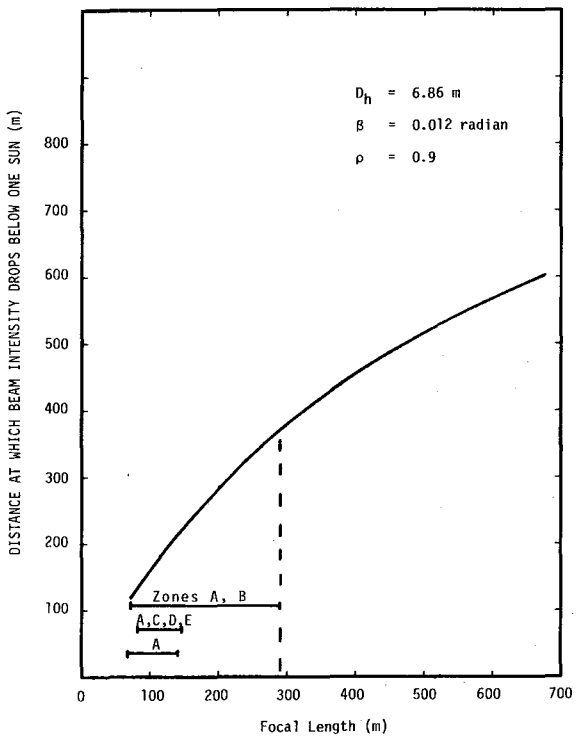

Figure 6. Distance at Which Single Beam Intensity Drops Below One Sun Versus Focal Length

Multiple Coincident Beams

Under normal operating conditions, all or most of the beams from active heliostats will converge on a receiver or other test item at the top of the tower, as illustrated in Figure 7. However, under certain conditions (e.g., intermittent clouds, flux rate-of-change experiments, or tests of the heliostat array without a receiver in place), some or all of the beams may be directed at a standby point (or points) in space near the top of the tower.

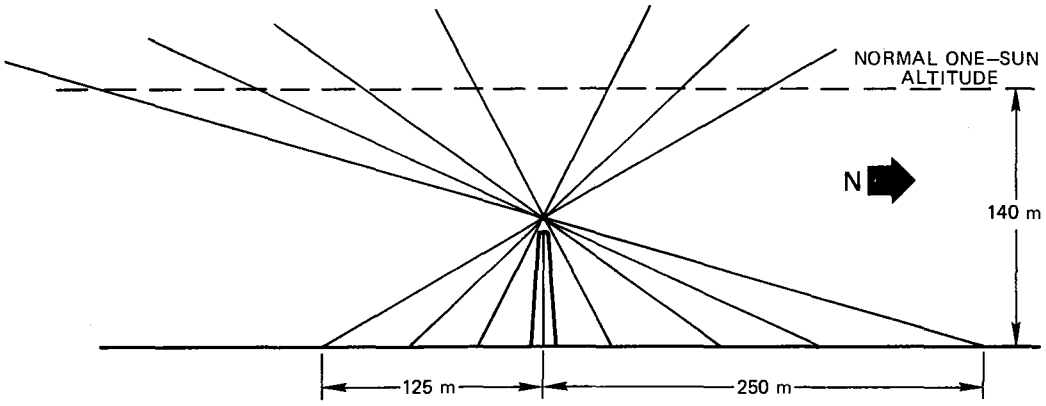

Figure 7. Heliostat Array Focusing Geometry

The flux density at or near the receiver location will reach 1000 to 1500 suns or possibly even higher in small regions. Above the focal zone, the beams will diverge from each other, and the flux density will drop rapidly. Assuming that all the heliostats are aimed at a single point in space near the top of the tower, the average flux density will be down to less than one sun at an altitude equal to about twice that of the aim point. Normally, this "safe" altitude would be about 120 to 140 meters above the field. However, there is also the possibility that two or more beams may be coincident at a higher altitude while they are being moved or if they are not aimed at the same point near the top of the tower. Under initial test facility plans, the motion of each heliostat was to be controlled so that its reflected beam would move by a safe route when being directed from face-down stowage to a receiver position (and similarly upon return). This was to assure that concentrated beams did not impinge on buildings, the tower, or other facilities in a manner which could endanger personnel or property.

However, this type of controlled movement is not necessarily sufficient to preclude possible coincidence of two or more beams at distant points in the sky.

The number of coincident beams required to produce a given total intensity I_t at a given distance will depend on the focal lengths of the heliostats involved. From Equation (2),

$$I_t = N\rho\left(\frac{1}{\frac{x\beta}{D_h} + \left|\frac{x}{b} - 1\right|}\right)^2$$

$$N = \frac{I_t}{\rho}\left(\frac{\beta x}{D_h} \quad \left|\frac{x}{b} - 1\right|\right)^2 \tag{5}$$

This relationship is shown for a one-sun intensity in Figure 8 for focal lengths of 100, 200, and 300 meters. Rearranging Equation (5), the distance at which a given number of heliostats of a given focal length could produce a given intensity is

$$x = \frac{(\rho N/I_t)^{0.5} + 1}{1/b + \beta/D_h} \qquad (x > b) \tag{6}$$

As shown by Figure 9, without explicit control to preclude distant multiple beam coincidence, the potential would exist for producing intensities greater than one sun at a considerable distance in the airspace above the facility.

Eye Hazard Thresholds

Retinal Burns

The maximum safe exposure level of the human eye to relatively high intensity light depends upon the wavelength, spectrum, source angle, and the duration of exposure.

For direct sunlight, the lowest intensity threshold is usually set by damage to the retina of the eye. Retinal exposure levels are shown in relation to a variety of sources in Figure 10 (taken from Sliney and Freasier[8]). Note that the maximum permissible (MPE) level decreases with increasing source angle (or retinal image size) up to about 5 degrees for a 0.15-second

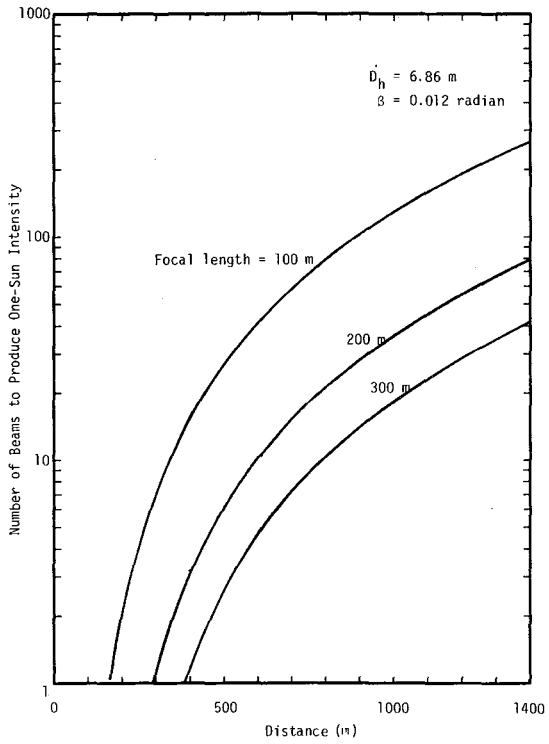

Figure 8. Number of Coincident Beams Required to Produce One-Sun Intensity

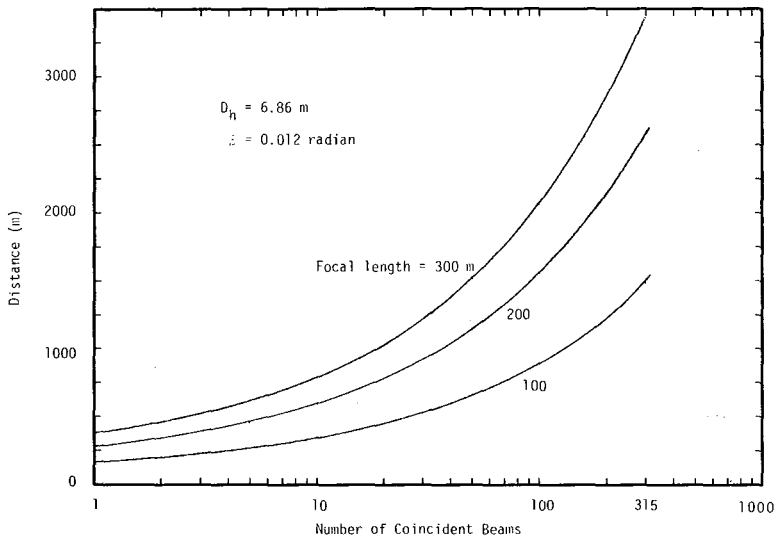

Figure 9. Distance at Which an Intensity of One Sun Could be Produced by a Given Number of Coincident Beams

exposure, which is typical of the human blink reflex time. Since the spectrum of the reflected beams is essentially the same as that of direct insolation, blink reflexes and the natural aversion to bright light would normally limit further retinal exposure at any level above about 10^{-4} W cm^{-2}.[8]

The geometry of the human eye is shown in Figure 11. The relationship between the irradiance at the cornea of the eye (E_c) and the retinal irradiance (E_r) for small source angles is [8,11]

$$L = \frac{E_c}{\Omega_s} = E_c\left(\frac{x^2}{A_L}\right) = E_c\left(\frac{f^2}{A_r}\right) \tag{7}$$

$$E_r = v\tau E_c A_c = \frac{v\tau E_c \pi d_p^2}{4} \tag{8}$$

$$E_r = \frac{\pi L v \tau d_p^2}{4f^2} \tag{9}$$

where

L = Source Radiance (W $cm^{-2}sr^{-1}$)

E_c = Corneal Irradiance (W cm^{-2})

Ω_s = Solid Angle of Source (sr)

A_L = Area of Source (m^2)

A_c = Area of Pupil (m)

x = Distance to Source (m)

A_r = Retinal Image Area (m^2)

d_p = Diameter of Pupil (m^2)

f = Focal Length of Eye $\approx$ 0.017 m

τ = Ocular Transmission $\approx$ 0.78

v = Fraction of Q between 400 and 1400 nm $\approx$ 0.62

The radiance of the sun on a clear day is about

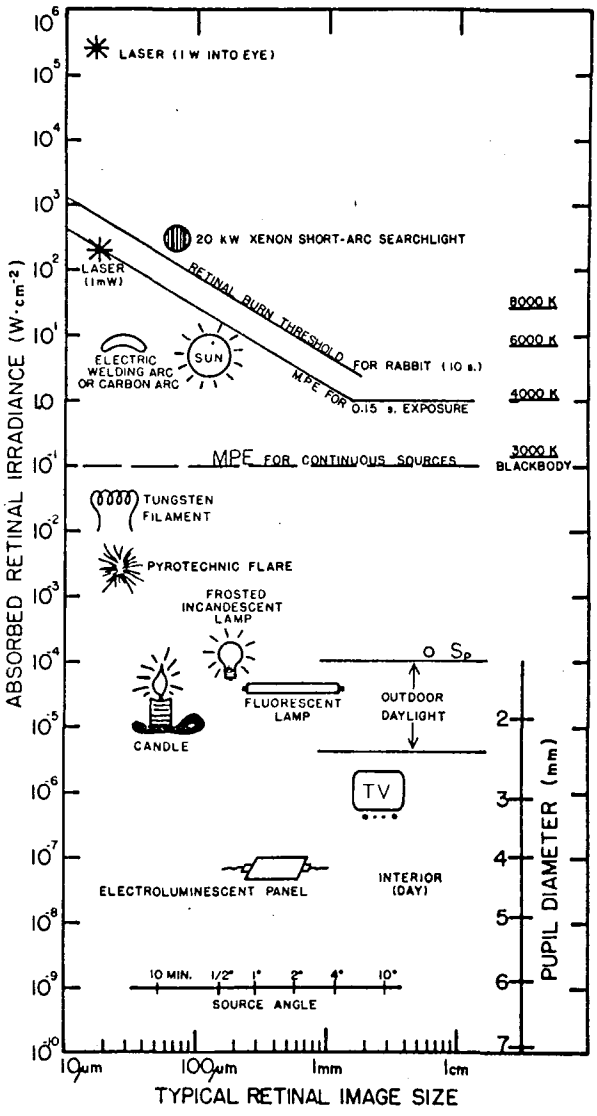

Note: The eye is exposed to light sources having radiances varying from ~10^4 W·cm^{-2}·sr^{-1} to ~10^{-6} W·cm^{-2}·sr^{-1} and less. The resulting retinal irradiances vary from ~200 W·cm^{-2} down to 10^{-7} W·cm^{-2} and even lower; retinal irradiances are shown for typical image sizes for several sources. A minimal pupil size was assumed for intense sources, except for searchlight. The retinal burn threshold for a 10-sec exposure of the rabbit retina[47] is shown as upper solid line. The maximum permissible exposure (MPE) applied by the U.S. Army Environmental Hygiene Agency in evaluating cw light sources is shown as lower solid line. Threshold for permanent shift of blue-cone sensitivity in monkeys obtained by Sperling is shown as O Sp at 3 x 10^{-4} W·cm^{-2}. Approximate pupil sizes are shown at lower right based upon exposure of most of the retina to light of the given irradiance. (Extracted from Sliney and Freasier[8])

Figure 10. Typical Light Sources and Eye Damage Thresholds

$$L_{sun} = \frac{Q}{\Omega_s} = \frac{0.11 \frac{W}{cm^2}}{\frac{\pi}{4}(0.0093)^2} = 1620 \frac{W}{cm^2 sr}$$

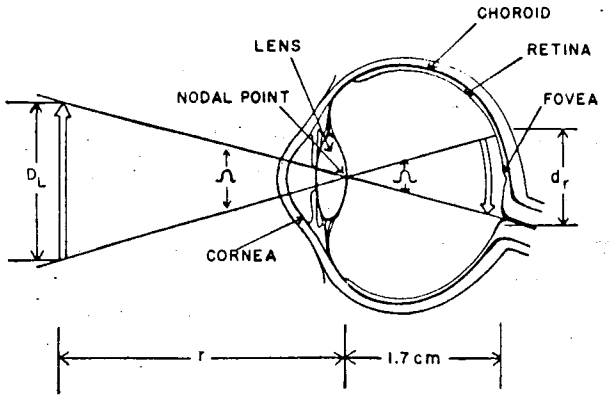

Note: An extended source is imaged at the retina; the approximate size of the image is determined using the simple geometric relation that both the object and image subtend an angle Ω measured at the eye's nodal point (~1.7 cm in front of the retina).

(Extracted from Sliney and Freasier.[8])

Figure 11. Geometry of the Human Eye

Within the transmission band of the eye (~400-1400 nm) the radiance is about 1000 W $cm^{-2}sr^{-1}$. At the retina, with a daylight adapted eye ($d_p \approx 2$ mm), this corresponds to

$$E_r = \frac{\pi v \tau d_p^2}{4f^2} L_{sun} = \frac{\pi(0.62)(0.78)(0.002)^2}{4(0.017)^2}(1620)$$

$$= 0.00525\ (1620) = 8.5\ W/cm^2 \qquad (10)$$

Because of conservation of brightness, the retinal irradiance resulting from a heliostat beam can be no higher than that resulting from direct viewing of the sun. However, retinal image size will depend on the distance to the heliostat, its size, and orientation, and the fraction of mirror area in which the sun's image is visible.

If one assumes an idealized mirror which has a perfectly specular surface (one which may attenuate but does not scatter reflected light) and which has a perfect paraboloidal shape, then the sun's image would appear

to completely fill the mirror when viewed from near the focal point with both the viewer and the sun on-axis. As the viewer moves away from the focal point (toward or away from the mirror), the sun's image would no longer fill the entire mirror. The effective source angle would then be that subtended by only the bright region.

Practical heliostats will of course not be perfectly specular or perfectly contoured, and rarely would the sun, heliostat and viewer be aligned on-axis. Consequently, the bright fraction of an unfilled heliostat will be somewhat larger, and the radiance will be somewhat lower and less uniform than in the idealized case above. Because a rigorous treatment of these variables is beyond the scope of this investigation, the radiance of a single heliostat will be assumed to be uniform and equal at all ranges to the value determined at its focal point. From Equations (2) and (7) for x = b,

$$E_c = \rho Q \left(\frac{D_h}{b\beta}\right)^2$$

$$\Omega_s = \frac{\pi}{4}\left(\frac{D_h}{b}\right)^2$$

$$L_{beam} = \frac{E_c}{\Omega_s} = \frac{4\rho Q}{\pi\beta^2} \tag{11}$$

$$= \frac{4(0.9)(0.11)}{\pi(0.012)^2} = 875\ \frac{W}{cm^2 sr} \tag{12}$$

The corresponding retinal irradiance is

$$E_r = 0.00525\ L_{beam} = 4.59\ \frac{W}{cm^2} \tag{13}$$

Note that at the focal point the retinal irradiance depends only on the mirror reflectivity and the total beam divergence (due to sun angle and mirror surface inaccuracies) and not upon the size or the particular focal length of a heliostat. The retinal irradiance value of 4.59 W/cm^2 is only about half of that which results from a momentary glance at the sun. Whether this level is safe, however, depends on the source angle and the resulting retinal image diameter.

Many standards for safe retinal exposure levels have been proposed to cover the wide variety of potential sources, conditions, and exposure times. The following expression for safe retinal irradiance (E_{rs}) as a

function of retinal image diameter is based on criteria proposed by Sliney and Freasier for circular images and a 0.15 second exposure.[8]

$$E_{rs} = \frac{0.002}{d_r} \text{ (W/cm}^2\text{)} \qquad (d_r \leqq 2 \times 10^{-3} \text{m}) \tag{14}$$

$$E_{rs} = 1 \text{ W/cm}^2 \qquad (d_r \geqq 2 \times 10^{-3} \text{m}) \tag{15}$$

where d_r = diameter of retinal image (m)

This expression gives values that are slightly more conservative than the MPE shown in Figure 10 and the values given in Table III of Reference 8 toward the lower end of the image diameter range. For momentary direct viewing of the sun (retinal image diameter = 0.158 mm) this expression gives a safe retinal irradiance of 12.7 W/cm^2, or about 1.5 times that which would actually occur. It is believed that under most circumstances there is probably an order of magnitude safety factor in this criteria.[8] This conservatism appears to be warranted, however, considering normal biological differences and uncertainties in current knowledge.

At the focal point of a heliostat, where the source angle is simply D_h/b, the focal length (b_s) at which the retinal irradiance equals the safe level can readily be determined.

$$d_r = f \frac{D_h}{b}$$

$$E_{rs} = \frac{0.002}{d_r} = 0.002 \frac{b}{fD_h}$$

$$E_r = 4.59 \text{ W/cm}^2$$

Setting $E_{rs} = E_r$

$$0.002 \frac{b_s}{f D_h} = 4.59$$

$$b_s = 39 D_h = 268 \text{ m} \tag{16}$$

Thus, any heliostat with a focal length greater than 268 m would not by itself be capable of producing an unsafe retinal irradiance at any distance.

At distances beyond or short of a heliostat's focal length, the image diameter and hence a safe retinal irradiance can be determined from the solid angle (Ω_s) which relates beam radiance to corneal irradiance.

$$\Omega_s = \frac{E_c}{L_{beam}}$$

$$\Omega = \left(\frac{4}{\pi}\,\Omega_s\right)^{0.5} = \left(\frac{4}{\pi}\,\frac{E_c}{L_{beam}}\right)^{0.5}$$

$$E_{rs} = \frac{0.002}{d_r} = \frac{0.002}{f\Omega} = \frac{0.002}{(0.017)\left(\frac{4E_c}{\pi(875)}\right)^{0.5}}$$

$$= 3.084\,E_c^{-0.5} = \frac{3.084}{(\rho Q_s)^{0.5}}\left(\frac{X\beta}{D_h} + \left|\frac{x}{b} - 1\right|\right) = 9.8\left(\frac{X\beta}{D_h} + \left|\frac{x}{b} - 1\right|\right) \qquad (17)$$

$$\frac{E_r}{E_{rs}} = \frac{0.469}{\frac{X\beta}{D_h} + \left|\frac{x}{b} - 1\right|} \qquad (18)$$

Retinal irradiance is shown relative to this safe limit in Figure 12. Note that the retinal irradiance of the 300 m focal length beam never exceeds the safe retinal limit, and that the 60, 100, and 200 m focal length beams exceed the safe limit for only a comparatively short distance (up to about 40 m) on either side of their respective focal points.

When the eye is exposed to multiple coincident beams, the flux density of each beam is additive at the outer surface of the cornea, but not at the retina. The total thermal power entering the eye and the irradiated retinal area both increase in accordance with the number of beams; but because the images do not overlap, the corresponding retinal irradiance does not increase.

If the eye is irradiated by two or more coincident beams from widely separated heliostats (e.g., 7 diameters or more), then each retinal image will also be well separated and surrounded by a much greater non-irradiated area. In this case, it seems reasonable to assume that each image is thermally independent for determination of safe levels for short duration exposures.

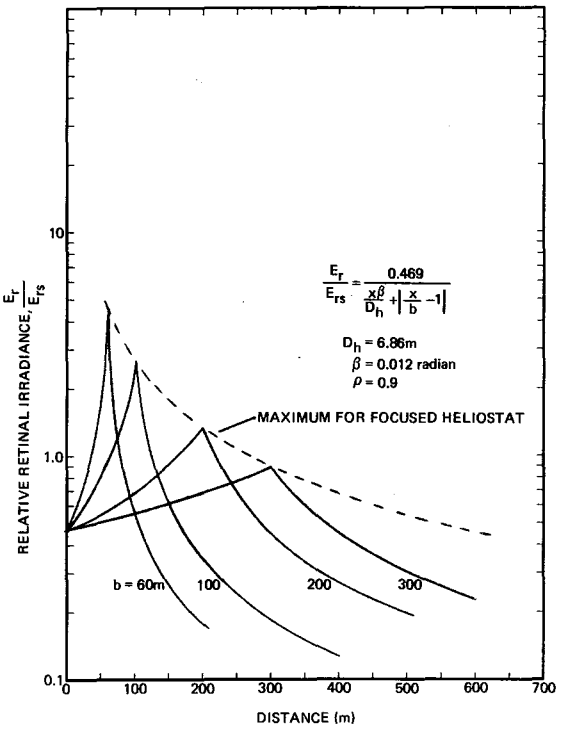

Figure 12. Single Beam Retinal Irradiance Relative to Safe Levels as a Function of Distance and Focal Length

In the case of coincident beams from immediately adjacent heliostats, however, the retinal images tend to coalesce into a continuous group and should probably be treated as a composite single image. Multiple coincident beams can thus pose a potential problem, not because the retinal irradiance is greater, but because the retina is less tolerant of the larger size of the composite image. This decreased tolerance is attributed to the greater temperature rise near the center of the image due to increasing limitations on heat dissipation as the image size increases. According to Table III of Reference 8, for purposes of determining safe retinal irradiance limits, the retinal images formed by a line of adjacent heliostats would be essentially equivalent to a circular group within the same source angle. The equivalent diameter of the composite retinal image (d_{rg}) can thus be expressed as

$$d_{rg} = \frac{fD_h}{x}\left(1 + \frac{N - 1}{K}\right) \tag{19}$$

where K = lineal spacing density = $\frac{D_h}{s}$

s = center-to-center spacing of adjacent heliostat beams near ground level (normal projection)

N_1 = number of coincident beams in line.

If N discrete images from an approximately circular group of heliostats are assumed to be coalesced into a single circular retinal image* (which would produce the greatest temperature rise on the retina), and using a constant beam radiance, the effective image diameter is

$$d_{gr} = f\,\Omega_g$$

$$L_{beam} = \frac{E_{gc}}{\Omega_{gs}} = 875\ \frac{W}{cm^2\,sr}$$

$$\Omega_g = \left(\frac{4}{\pi}\ \Omega_{gs}\right)^{0.5}$$

$$d_{gr} = f\left(\frac{4}{\pi}\,\Omega_{gs}\right)^{0.5} = f\left(\frac{4}{\pi}\,\frac{E_{gc}}{L_{beam}}\right)^{0.5}$$

$$= 6.48 \times 10^{-4}\ E_{gc}^{0.5} \tag{20}$$

$$d_{gr} = 6.48 \times 10^{-4}\ \frac{(N\rho Q)^{0.5}}{\frac{x\beta}{D_h} + \left|\frac{x}{b} - 1\right|} \tag{21}$$

From Equation (13) the retinal irradiance which corresponds to a beam radiance of 875 W $cm^{-2}sr^{-1}$ is 4.59 W cm^{-2}. From Equation (14), the corresponding maximum safe retinal image diameter is

$$d_{rs} = \frac{0.002}{4.59} = 4.357 \times 10^{-4}\ m \tag{22}$$

By setting $d_{gr} = d_{rs}$, the number of beams necessary to produce an effective image diameter equal to d_{rs} can be determined.

$$d_{rs} = d_{gr}$$

$$\frac{4(0.002)f^2}{\pi v \tau d_p^2\, L_{beam}} = f\left(\frac{4\ N_s\ E_c}{\pi\ L_{beam}}\right)^{0.5}$$

*This assumes the projected area density ψ is equal to one; situations where ψ is less than one are discussed later.

$$N_s = \frac{5.093 \times 10^{-6}}{E_c L_{beam}} \left(\frac{f}{v\tau d_p}\right)^2$$

$$N_s = 4 \times 10^{-6} \left(\frac{f}{v\tau d_p^2}\right)^2 \left(\frac{\beta}{\rho Q}\right)^2 \left(\frac{x\beta}{D_h} + \left|\frac{x}{b} - 1\right|\right)^2 \quad (23)$$

$$N_s = 4.539 \left(\frac{x\beta}{D_h} + \left|\frac{x}{b} - 1\right|\right)^2 \quad (24)$$

This relationship is shown in Figure 13.

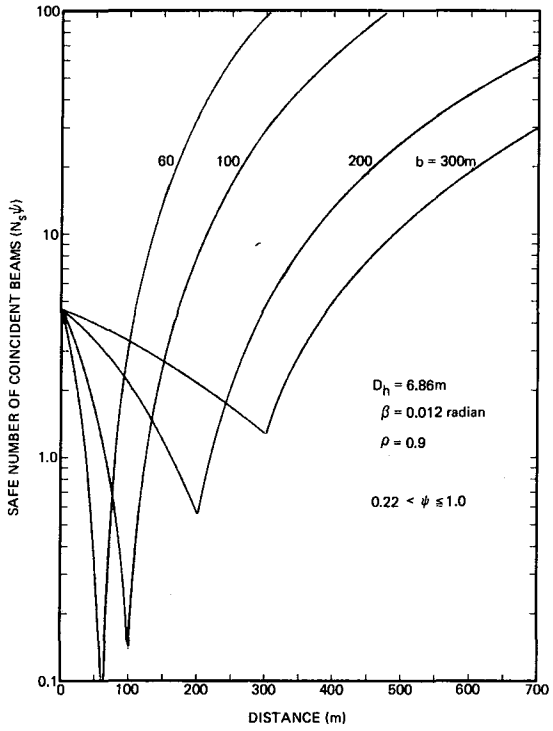

Figure 13. Number of Adjacent Beams Corresponding to Safe Retinal Irradiance as a Function of Distance, Focal Length and Projected Area Density

Figure 13 can also be applied to groups of discrete images, where the projected area density ψ is less than one, if the correspondingly lower average retinal irradiance is used. On the retina, the average retinal irradiance over the region occupied by a group of images is directly proportional to ψ.

$$E_{gr} = E_r \psi = 4.59\,\psi \ (W/cm^2) \quad (25)$$

The maximum safe image diameter corresponding to this average irradiance is

$$d_{grs} = \frac{0.002}{4.59\,\psi} \qquad (\text{For } 0.22 < \psi < 1.0) \tag{26}$$

Since the area of a group of retinal images is inversely proportional to ψ, the diameter of a circular group will be

$$d_{gr} = \frac{1}{\psi^{0.5}}\, d_{ger}$$

$$= \frac{6.48 \times 10^{-4}}{\psi^{0.5}} \frac{(N\rho Q)^{0.5}}{\frac{x\beta}{D_h} + \left|\frac{x}{b} - 1\right|} \tag{27}$$

Setting $d_{gr} = d_{grs}$

$$\frac{6.48 \times 10^{-4}}{\psi^{0.5}} \frac{(N\rho Q)^{0.5}}{\frac{x\beta}{D_h} + \left|\frac{x}{b} - 1\right|} = \frac{0.002}{4.59\,\psi}$$

$$\psi N_s = 4.539 \left(\frac{x\beta}{D_h} + \left|\frac{x}{b} - 1\right|\right)^2 \tag{28}$$

The distance (x_s) at which a given number of coincident beams would drop below the retinal MPE can similarly be determined by rearranging the foregoing expression.

$$x_s = \frac{0.469\,(N\psi)^{0.5} + 1}{\frac{\beta}{D_h} + \frac{1}{b}} \tag{29}$$

Since Equation (28) is a more general form of Equation (24) (in which ψ was assumed to be one), the ordinate of Figure 13 can now be shown as the product $N\psi$.

It should be noted, however, that when used with values of ψ less than one, the results may tend to be less conservative. This is because the relationship in such cases is based on the average irradiance over the retinal region occupied by a group of higher intensity discrete images; there is little biological information available to judge how this type of exposure compares to a uniform irradiance equal to the average.

Additional conservatism can be inserted by assuming values of ψ somewhat higher than is actually the case or, to bound the problem, by assuming ψ to be equal to one.

Figure 13 is also very useful for determining the retinal irradiance relative to the MPE (i.e., the margin of safety). The average retinal irradiance over the region occupied by a group of discrete images is given by

$$E_{gr} = 4.59\,\psi \quad (W/cm^2) \tag{30}$$

The safe retinal irradiance is

$$E_{grs} = \frac{0.002}{d_{gr}} = \frac{0.002}{f}\left(\frac{\pi\psi L_{beam}}{4\,NE_c}\right)^{0.5}$$

$$= 9.8\left(\frac{\psi}{N}\right)^{0.5}\left(\frac{x\beta}{D_h} + \left|\frac{x}{b} - 1\right|\right) \tag{31}$$

and the ratio of E_{gr} to E_{grs} is

$$\frac{E_{gr}}{E_{grs}} = 500\,\frac{\rho Q v \tau d_p^2}{f\beta}\,\frac{(N\psi)^{0.5}}{\frac{x\beta}{D_h} + \left|\frac{x}{b} - 1\right|} \tag{32}$$

$$= 0.469\,\frac{(\psi N)^{0.5}}{\frac{x\beta}{D_h} + \left|\frac{x}{b} - 1\right|} = \frac{(\psi N)^{0.5}}{2.13\left(\frac{x\beta}{D_h} + \left|\frac{x}{b} - 1\right|\right)} \tag{33}$$

Note that the denominator of this expression is equal to the square root of ψN_s as shown in Equation (28). Therefore,

$$\frac{E_{gr}}{E_{grs}} = \frac{(N\psi)^{0.5}}{(N_s\psi)^{0.5}} = \left(\frac{N}{N_s}\right)^{0.5} \tag{34}$$

Thus, the retinal irradiance, relative to the safe level, can be readily determined from Figure 13 for any value of N. At a distance of 500 m, for example, about 10 coincident 300 m focal length beams would be required to produce the maximum permissible retinal exposure. The relative retinal irradiance produced by twice as many beams at that distance would be

$$\frac{E_{gr}}{E_{grs}} = \left(\frac{20}{10}\right)^{0.5} = 1.4$$

Similarly, 4 beams would produce a relative irradiance of 0.63.

As another example, what would be the relative retinal irradiance for a group of 15 beams of 200 m focal length at a distance of 300 m if the projected area density were 0.75?

At 300 m, $N_s\psi = 5$ (from Figure 13)

$$N_s = \frac{5}{0.75} = 6.7$$

and

$$\frac{E_{gr}}{E_{grs}} = \left(\frac{15}{6.7}\right)^{0.5} = 1.5$$

Distractive Glint

Probably the most common glint effects experienced by pilots are those due to sunlight reflected from bodies of water. The intensity of such reflected light can vary considerably, depending on the water surface wave condition and the sun elevation angle. As indicated by the curve labeled "External" in Figure 14, the reflectivity of a smooth water surface is only a few percent for angles of incidence up to about 50 degrees and rises above 20 percent only for angles greater than about 75 degrees.[9] For increasing angles of incidence above 75 degrees (sun elevation angles less than 15 degrees), direct insolation decreases rapidly due to atmospheric attenuation. In the case of a very quiet, smooth water surface, the reflected light would undergo comparatively little scattering.

For bodies of water in which the entire reflected image of the sun can be seen, the intensity at a distance x depends primarily on the wave condition of the water surface. For a large, perfectly smooth, specular surface, the intensity would simply be:

$$I = \rho_\theta Q$$

where

Q = the direct normal insolation

ρ_θ = the specular reflectivity of the surface at the incidence angle θ

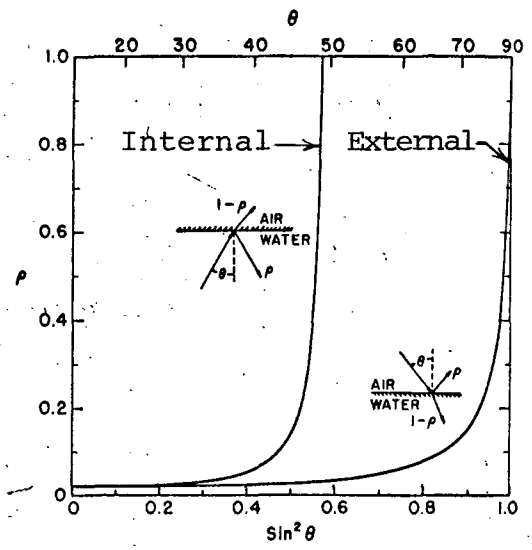

(Excerpted from Viskanta and Toor[9])

Figure 14. Reflectance of the Atmosphere-Water Interface as a Function of the Angle of Incidence for External and Internal Reflections

For angles of incidence less than about 50 degrees, the intensity would be no greater than about 0.03 suns[9] and for this case would be essentially independent of distance. Under actual conditions, however, water surfaces are seldom perfectly smooth, and the reflected intensity would usually be considerably lower because of scattering.

The distance at which comparable intensities could be produced by coincident beams from test facility heliostats can be readily determined from Equation (6). As an example, Figure 15 shows intensity versus distance for 5 coincident beams. Note that the maximum glint intensity at 2600 meters (from 5 coincident, 300-meter focal length beams) is about equal to the maximum intensity reflected from bodies of water. At greater distances, the intensity would continue to decrease and be roughly comparable to levels normally experienced by aircraft personnel. Although the retinal irradiance would be higher, the image diameter would be somewhat smaller.

Control Measures

Based upon the potential light intensities derived for multiple beam coincidence and the established maximum safe exposure level of the human eye, it was apparent that some form of additional protection should be instituted to insure that the light intensities produced would not pose a safety problem. Two basic types of control were considered: exclusion zones and beam control methods.

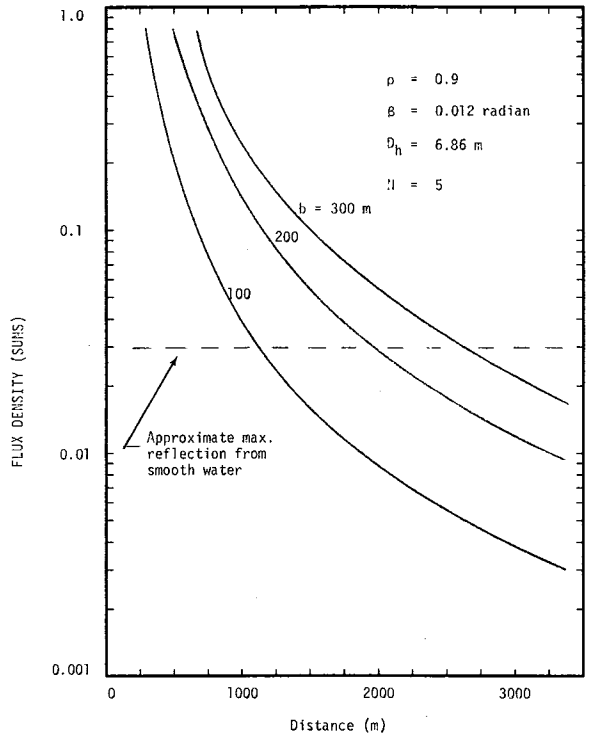

Figure 15. Flux Density of Five Coincident Beams Versus Distance

Exclusion Zones

If an exclusion zone were to be established to protect against a worst-case random coincidence of uncontrolled beams from all of the heliostats, it might have to extend as high as 2700 meters (~9000 feet) above the facility (assuming 315 beams with 200-meter mean focal length and a one-sun intensity). Use of such an extreme criteria would hardly be justified, however, since momentary coincidence of all the beams at the precise location and time of passage of an overflying aircraft would be very improbable--even if no special control over beam movement is assumed. On the other hand, the frequency of momentary coincidence of smaller groups of adjacent heliostats could be high enough to be of concern.

Figure 16 shows the exclusion zones which would be required to protect against groups of 2, 5, 10, 20, and 30 coincident beams. Beams with 300-meter focal lengths from near the north end of the field are shown, since they represent the worst case. Note that one-sun exclusion zones for even these comparatively small groups of coincident beams would extend to considerable altitudes (e.g., ~800 meters for 10 beams and 1200 meters for 30 beams).

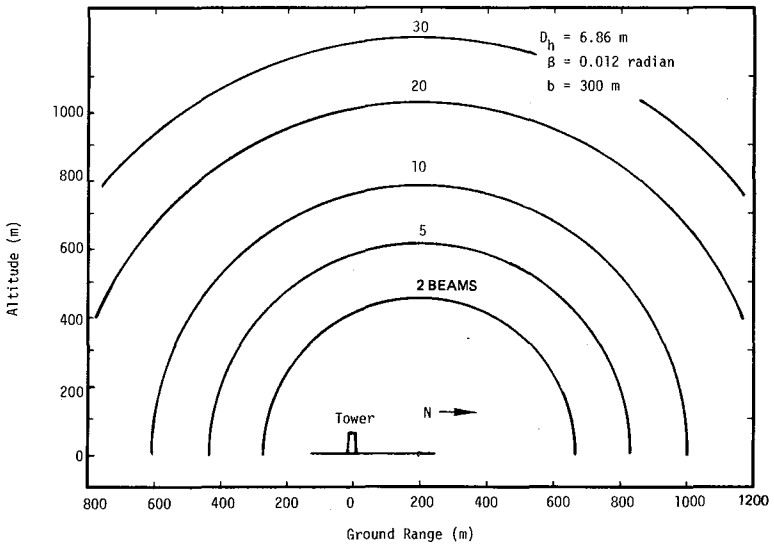

Figure 16. Hemispherical Exclusion Zones Based on One Sun Intensity for Multiple Coincident Beams

If maximum safe retinal exposure is used as the criteria [Equation (29)], exclusion zones shrink considerably from those corresponding to a one-sun criteria, but they still extend to comparatively high altitudes for moderate numbers of coincident beams (Figure 17). Consequently, it appeared that some form of heliostat beam control was warranted to preclude potentially unsafe exposures at normal aircraft altitudes.

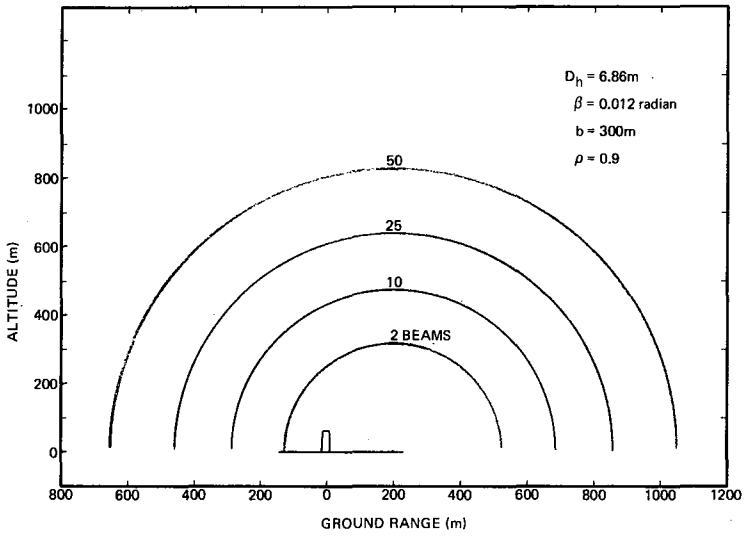

Figure 17. Hemispherical Exclusion Zones Based on Maximum Permissible Retinal Exposure for Multiple Coalesced Beams

Beam Control Techniques

As a result of the foregoing analyses, it became evident that additional beam control measures were desirable so that potentially unsafe intensities would not extend to excessively high altitudes. Three of the various approaches considered are described below.

Aircraft Proximity Method--One early suggestion was to move the heliostats only when no aircraft were in the vicinity of the test facility. This method would impose constraints on heliostat movements so that reflected beams were always aimed either below the horizon or at a common point near the top of the tower when aircraft were within a certain range. This would require visual observation or radar surveillance of the surrounding air space prior to and during beam movements.

One recognized difficulty with this approach was the need to anticipate the course of aircraft so as to assure that the heliostat beams were not "enroute" to or from the aim point when an aircraft entered the potentially hazardous zone. The heliostat specification allows up to 15 minutes for beam movements between face-down stowage and target positions. Assuming beams are above the horizon for only half of this interval, this time for beam movement translates into a range of 25 to 50 miles at aircraft speeds of 200 to 400 miles per hour. Predicting aircraft movements to this extent would certainly be vexing, if not impossible. In the event of an unanticipated intrusion, simply stopping the heliostats or instigating emergency stow would not preclude the possibility of unsafe exposures. In addition to the foregoing difficulties, this approach would also impose undesirable constraints on facility test operations.

Beam Divergence Method--A second and seemingly more practical approach was to control heliostat movements in such a way that no more than a specified number of beams could coincide beyond a specified distance or altitude. This control could be accomplished by moving individual or small groups of heliostats in sequence so as to maintain some minimum angular divergence (including zero) between beams. For example, the heliostats might be moved from the receiver to their standby positions by sequentially "peeling off" outermost beams until all the mirrors were parallel or in slightly divergent orientations; the heliostats could then be moved in unison to a face-down or other stow position. (There would of course still be instances when some or all of the beams would be aimed at a "standby point" near the top of the tower.) While this beam divergence method seemed to be one of the simplest approaches, the time involved in the sequential movement of heliostats tended to be excessive. These times could be reduced considerably, but only at the expense of adding more complexity to the control system.

Convergence/Divergence Method--Another way of maintaining beam divergence in the distant airspace was to bring a group of beams up simultaneously to a standby point near the receiver by keeping all of the beams aimed at a common, mobile point which moves in a programmed manner from the ground to the standby point. To illustrate, visualize an imaginary target which slides up (or down) a "wire" stretched from the standby point to a ground anchor point located in front or off to one side of the group of mirrors being moved. The "bundle" of beams converges on the target and remains focused on the target as it moves up the wire; beyond the target point, the beams diverge from each other. The advantages of this approach are: (1) the maximum elevation angle of each beam is limited, (2) the beams within each group diverge from each other beyond the aim point, and (3) the number of potentially coincident beams in the distant airspace* is no greater than the number of beam groups. Because this approach was the most compatible with the control system under development and with other test facility requirements, it was ultimately incorporated into the control system design.

In areas where beam groups are aimed at two or more points along the same wire, the only potentially coincident beams in the distant airspace are those from heliostats in different groups which lie in a common plane with the wire. For example, a beam from any given heliostat in Group A is potentially coincident only with beams from those heliostats in a different group (B) which lie along a line between the reference Group A heliostat and the bottom end of the wire. Some or all of the beams from this subset of Group B may successively coincide with the Group A heliostat beam, but never more than two would be simultaneously coincident.

This beam control method, along with judicious selection of the "wire," effectively limits the elevation angle of any heliostat beam to that necessary to reach the test zone at the top of the tower. Consequently, there will be a limiting altitude (y) corresponding to a distance x from the heliostat along the beam.

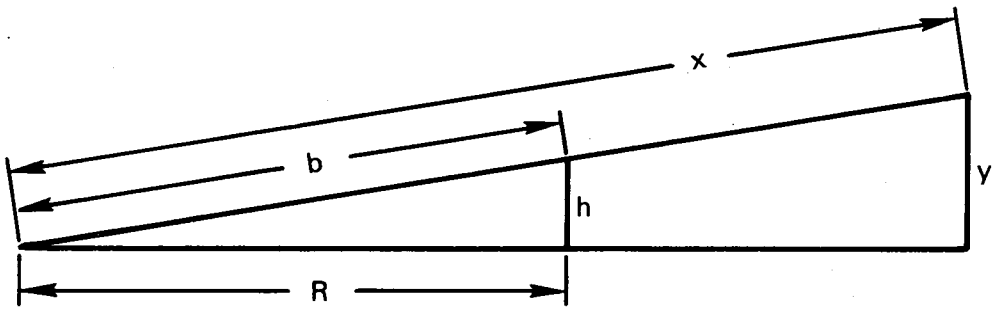

*Beyond the distance at which adjacent beams disengage; this disengagement distance is treated later.

For this configuration,

$$\frac{y}{h} = \frac{x}{b}$$

where

h = height to the receiver or standby point (whichever is higher)

R = ground radius from base of tower to heliostat

b = heliostat focal length (assumed equal to slant range to the receiver)

Substituting in Equation (6),

$$y = \left(\frac{h}{b}\right) \frac{\left(\frac{\rho N}{I}\right)^{0.5} + 1}{\frac{\beta}{D_n} + \frac{1}{b}} \qquad (x > b) \qquad (35)$$

Equation (35) thus gives the altitude at which a given number of coincident beams of a given focal length could produce a certain intensity subject to the foregoing limitation on maximum elevation angle. This relationship is shown in Figure 18 for a one-sun intensity and a maximum target height of 70 m. Note that in contrast to the foregoing cases in which beams were not constrained in elevation angle, the one-sun altitudes are much lower and are determined by the short rather than long focal length beams. Rearranging Equation (35), the number of beams required to produce a given intensity at an altitude y is

$$N = \frac{I}{\rho}\left[\frac{y}{h}\left(\frac{b\beta}{D_h} + 1\right) - 1\right]^2 \qquad (36)$$

The number of coincident beams required to produce the maximum permissible retinal exposure (MPE) can also be determined with this elevation angle limitation by substitution into Equation (28).

$$x = \frac{b}{h} y$$

$$\psi N_s = 4.539\left(\frac{by\beta}{h D_h} + \left|\frac{y}{h} - 1\right|\right)^2 \qquad (37)$$

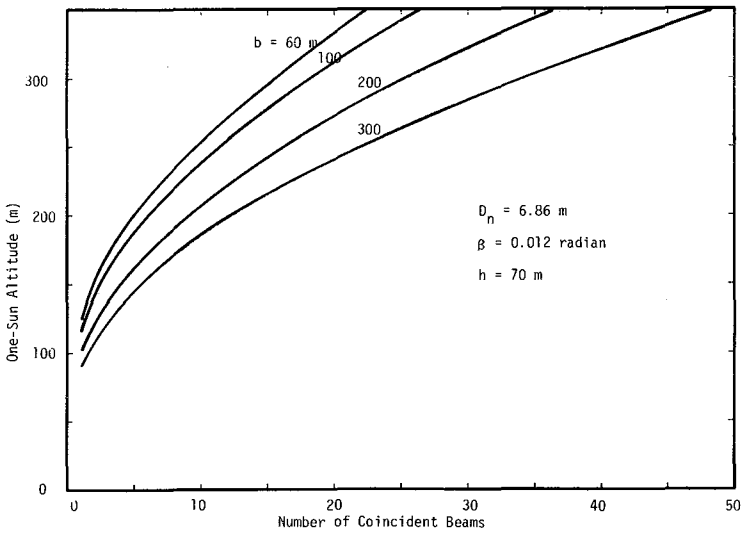

Figure 18. Altitude at Which a One-Sun Intensity Could be Produced by a Given Number of Coincident Beams With Elevation Angle Limitation

$$\frac{E_{gr}}{E_{grs}} = \left(\frac{N}{N_s}\right)^{0.5} \tag{38}$$

The relationship of Equation (37) is shown in Figure 19. Note that the fewest number of beams capable of producing an MPE are those from the shortest focal length heliostats. This is reversed from the situation shown in Figure 13 (where the maximum safe number is expressed as a function of distance) and is a direct result of the elevation angle limitation.

Rearranging Equation (37), the altitude (y_s) at which the retinal irradiance drops to a safe level is

$$y_s = \frac{h[0.469\ (N\psi)^{0.5} + 1]}{\frac{b\beta}{D_h} + 1}$$

Figure 20 shows this relationship for $\psi = 1$.

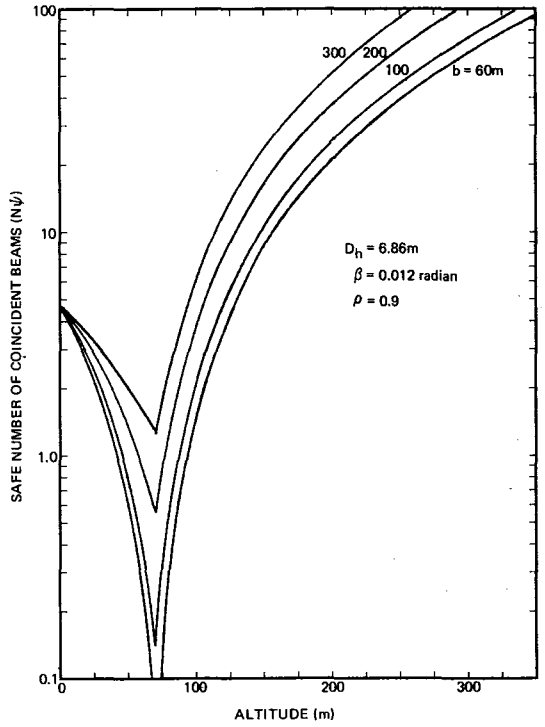

Figure 19. Number of Coincident Beams Corresponding to Safe Retinal Irradiance as a Function of Altitude, Focal Length and Projected Area Density With Elevation Angle Limitation

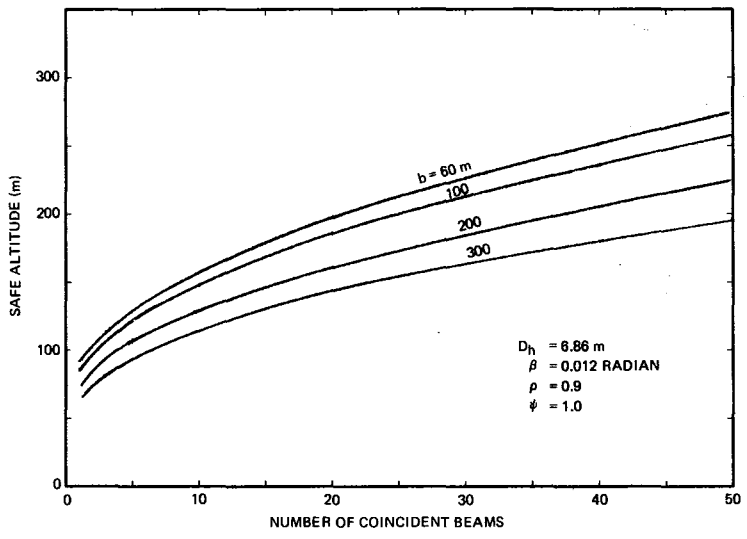

Figure 20. Altitude at Which Retinal Exposure Drops to a Safe Level as a Function of Number of Coincident Beams With Elevation Angle Limitation

An important additional advantage of elevation angle limitation is evident by comparing Figure 19 to Figure 13.* With the angle limitation, altitude limits are greatly reduced for all but the shortest focal length beams. Note for example that without angle limitation, 20 coincident beams could produce an MPE at 600 m altitude (Figure 13); with elevation angle limitation (Figure 19), 20 beams could produce an MPE at only 200 m.

Beam Disengagement--Even though the central rays of beams in a given group will diverge beyond the aim point, each beam will also be expanding. If two adjacent beams diverge from each other at a rate greater than each beam expands, then the beams will disengage at some distance x_d when the separation (w) of the central rays is equal to the beam diameter.

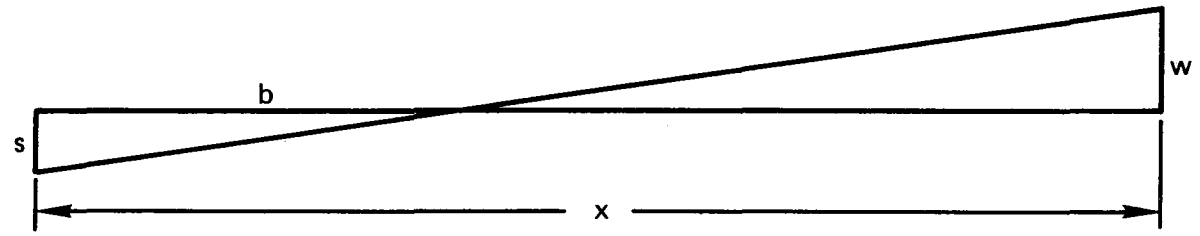

Figure 21. Beam Disengagement Geometry With Zero Tracking Error

From Figure 21, assuming perfect tracking,

$$\frac{w}{s} = \frac{x - b}{b}$$

$$w = s\left(\frac{x}{b} - 1\right)$$

where

s = center-to-center spacing of two adjacent heliostats

b = focal length of beams (and in this case the distance at which the central rays intersect)

*In the absence of a specific beam control method, Figure 13 obviously applies to both distance and altitude.

From Equation (1), the beam diameter is

$$D_x = 2\,R_x = x\beta + \left(\frac{x}{b} - 1\right) D_h$$

Setting w equal to D_x

$$s\left(\frac{x_d}{b} - 1\right) = x_d\beta + \left(\frac{x_d}{b} - 1\right) D_h$$

$$x_d = \frac{D_h - s}{\beta + \frac{D_h - s}{b}} = \frac{b(D_h - s)}{b\beta + D_h - s} \tag{39}$$

x_d is thus the distance at which two adjacent beams disengage. The value of s below which adjacent beams will never completely disengage (s_0) can be determined by setting $x_d = \infty$, which yields

$$s_0 = D_h + b\beta \tag{40}$$

The disengagement altitude (y_d) is given by

$$y_d = \left(\frac{h}{b}\right) \frac{D_h - s}{\beta + \frac{D_h - s}{b}}$$

$$y_d = \frac{h(D_h - s)}{D_h + b\beta - s} = \frac{h(D_h - s)}{s_0 - s} \tag{41}$$

This relationship is shown in Figure 22.

Because of tracking errors, the central rays of beams will not intersect exactly at the aim point. Consequently, beams which intersect beyond the aim point will disengage at a somewhat greater altitude than indicated by the preceeding analysis which assumed perfect aiming. From Figure 23, an assumed maximum angular error between two beams results in a separation (e) of the central rays at the aim point and a separation (w) at a distance x.

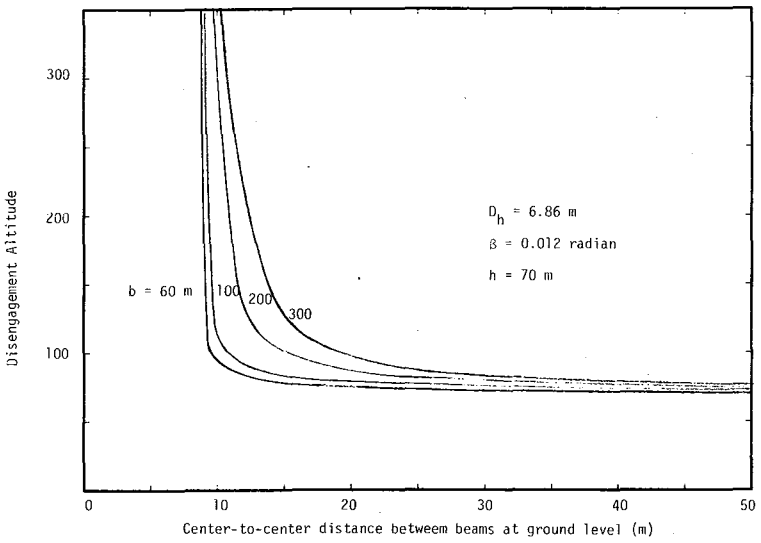

Figure 22. Altitude at Which Two Adjacent Beams of a Given Separation and Focal Length Disengage With Elevation Angle Limitation and Zero Tracking Error

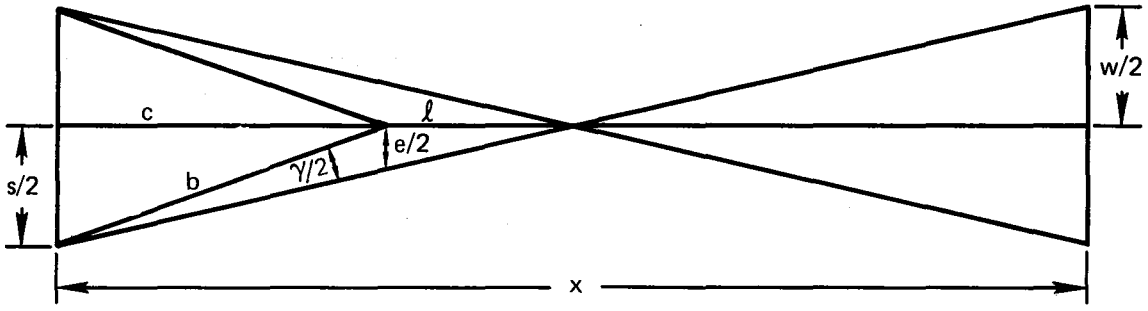

Figure 23. Beam Disengagement Geometry Considering Tracking Errors

$$\frac{w}{s} = \frac{x - (\ell + c)}{\ell + c} = \frac{x}{\ell + c} - 1$$

$$\frac{e}{\ell} = \frac{s}{\ell + c}$$

$$\ell = \frac{ec}{s - e}$$

Substituting

$$\frac{w}{s} = \frac{x}{\frac{ec}{s - e} + c} - 1 = \frac{x(s - e)}{cs} - 1$$

For $b >> s$, $b \approx c$

$$\frac{w}{s} = \frac{x(s - e)}{sb} - 1$$

$$w = s\left(\frac{x}{b} - 1\right) - \frac{ex}{b}$$

For small values of γ

$$e = b\gamma$$

$$w = s\left(\frac{x}{b} - 1\right) - \gamma x$$

The degree of disengagement can be expressed by dividing w by the beam diameter D_x (Equation (1)).

$$\frac{w}{D_x} = \frac{s\left(\frac{x}{b} - 1\right) - \gamma x}{x\beta + \left(\frac{x}{b} - 1\right) D_h}$$

$$\frac{w}{D_x} = \frac{(s - b\gamma)\, x - bs}{(b\beta + D_h)\, x - b\, D_h} \qquad (42)$$

The distance at which two beams disengage (x_d) is determined by setting $w/D_x = 1$.

$$1 = \frac{s\left(\frac{x_d}{b} - 1\right) - \gamma x_d}{\beta x_d + \left(\frac{x_d}{b} - 1\right) D_h}$$

Collecting and rearranging terms,

$$x_d = \frac{b(D_h - s)}{b(\beta + \gamma) + D_h - s}$$

$$s_0 = b(\beta + \gamma) + D_h \tag{43}$$

$$x_d = \frac{b(D_h - s)}{s_0 - s} \tag{44}$$

Similarly, for any distance, the beam separation s_d beyond which all beams will have disengaged can be expressed as

$$s_d = \frac{s_0 x - b D_h}{x - b} \tag{45}$$

Equations (42), (44), and (45) can also be expressed in terms of altitude instead of distance.

$$\frac{w}{D_x} = \frac{(s - b\gamma)\, y - hs}{(b\beta + D_h)\, y - h\, D_h} \tag{46}$$

$$y_d = \frac{h\,(D_h - s)}{s_0 - s} \tag{47}$$

$$s_d = \frac{s_0 y - h\, D_h}{y - h} \tag{48}$$

Disengagement altitude is shown in Figure 24 for a tracking error of ±10 mrad (γ = 20 mrad), which corresponds to the STTF tracking accuracy specification for beam control in this mode of operation. Note that the longest focal length beams have the highest disengagement altitudes.

The center-to-center ground spacing of the test facility heliostats is variable and ranges from about 9.75 to 26 m. However, because of the geometric arrangement, the center-to-center spacing between adjacent

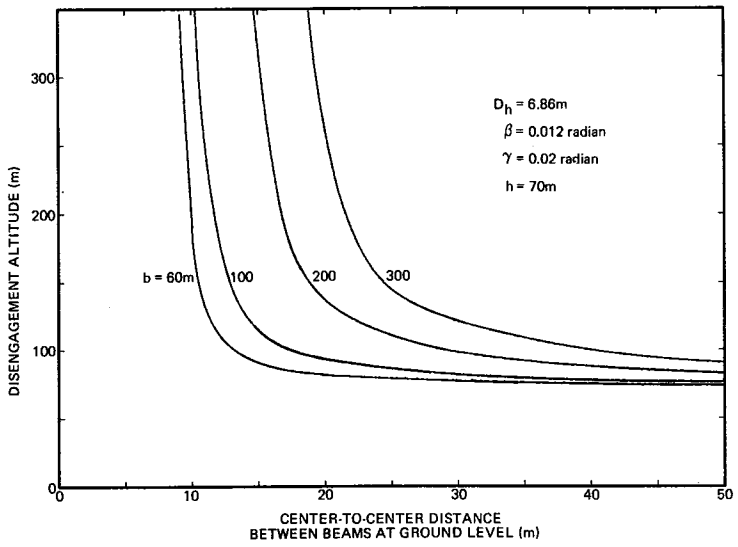

Figure 24. Altitude at Which Two Adjacent Beams of a Given Separation and Focal Length Disengage With Angle Limitation and ±10 Milliradian Tracking Error

reflected beams (in the orthogonal projection) is less and ranges from about 6.9 to 10 m. It is evident from Figure 24 that, except for a few short focal length beams, any adjacent pair of beams may never completely disengage. Consequently, any assessment of flux versus altitude must consider both the decreasing intensity of each beam and the progressive disengagement of other beams in a "bundle."

The following example illustrates the coupled effects. Figure 25 is a projection of adjacent beams in a plane normal to a reference beam from a heliostat 195 m north of the tower. The beams are directed at a point 70 m above the ground on the centerline of the tower. The circular boundaries shown in Figure 25 are useful in determining how many and which heliostats are potentially coincident at various altitudes. Heliostats which are outside a given circle* will disengage from the central reference beam below the indicated altitude. Thus, heliostats 2 through 9 will never completely disengage from heliostat 1. However, this does not mean that they all remain mutually coincident. Heliostat 10 disengages somewhere above 200 m, heliostat 11 at 200 m, and heliostats 12 through 15 each disengage from No. 1 between 140 and 200 m.

*Radii of the circles are determined from Equations (43) and (48c) for γ = 0.02 radian.

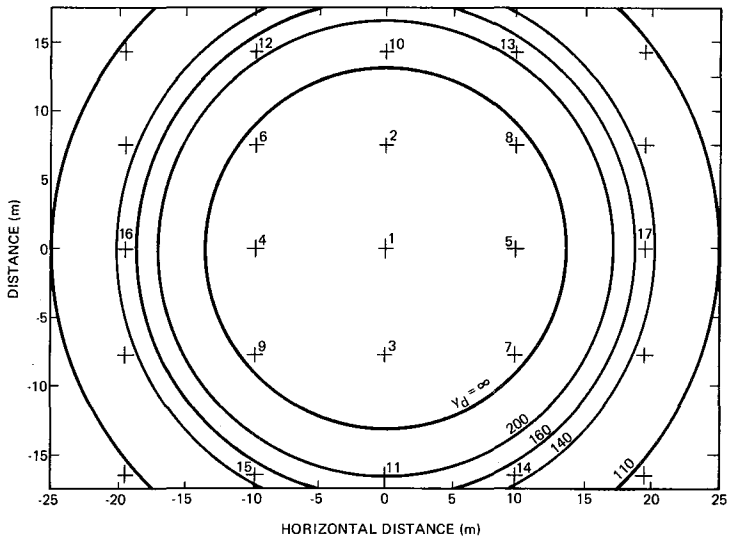

Figure 25. Normal Projection of Beams Surrounding a Reference Heliostat 195 m North of the Tower

Stated in a somewhat more useful way, each circle in Figure 25 encompasses all of the heliostats which are potentially coincident with each other above the indicated altitude. For any altitude of interest, therefore, the number and location of all of the heliostats which must be considered can readily be determined; the rest can be neglected.

Figure 26 shows the cumulative number of potentially coincident beams as a function of center-to-center distance from the reference beam. Figure 27 shows a succession of cross sections of the reference beam along with its nine nearest neighbors as the beams expand and diverge from each other with increasing altitude. The series on the left is for perfect tracking; the series on the right is for a coarse tracking error of ±10 milliradian. Note that the maximum intensities occur in localized regions where the maximum number of beams overlap. The resultant maximum intensity drops rapidly with increasing altitude because of the combined effects of beam disengagement and the decreasing intensity of each beam. Note also that with tracking error, more beams can remain engaged to higher altitudes.

Adding additional beams to a group will of course increase the number of coincident beams and the total intensity in direct proportion to the number of beams for altitudes near the focal point. However, above a certain altitude (about 200 m in this example) adding more beams to the group would not increase the number of coincident beams because they would disengage from the reference beam at a lower altitude. The multiple beam intensity in

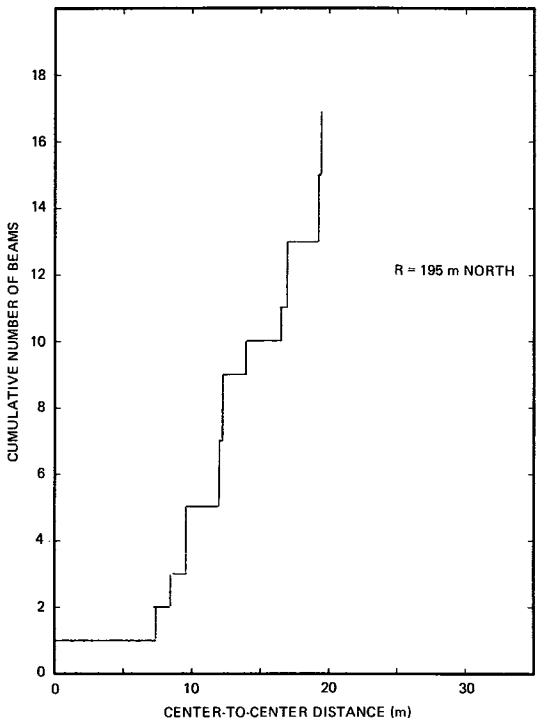

Figure 26. Cumulative Number of Beams as a Function of Center-to-Center Distance From a Heliostat Beam 195 m North of Tower

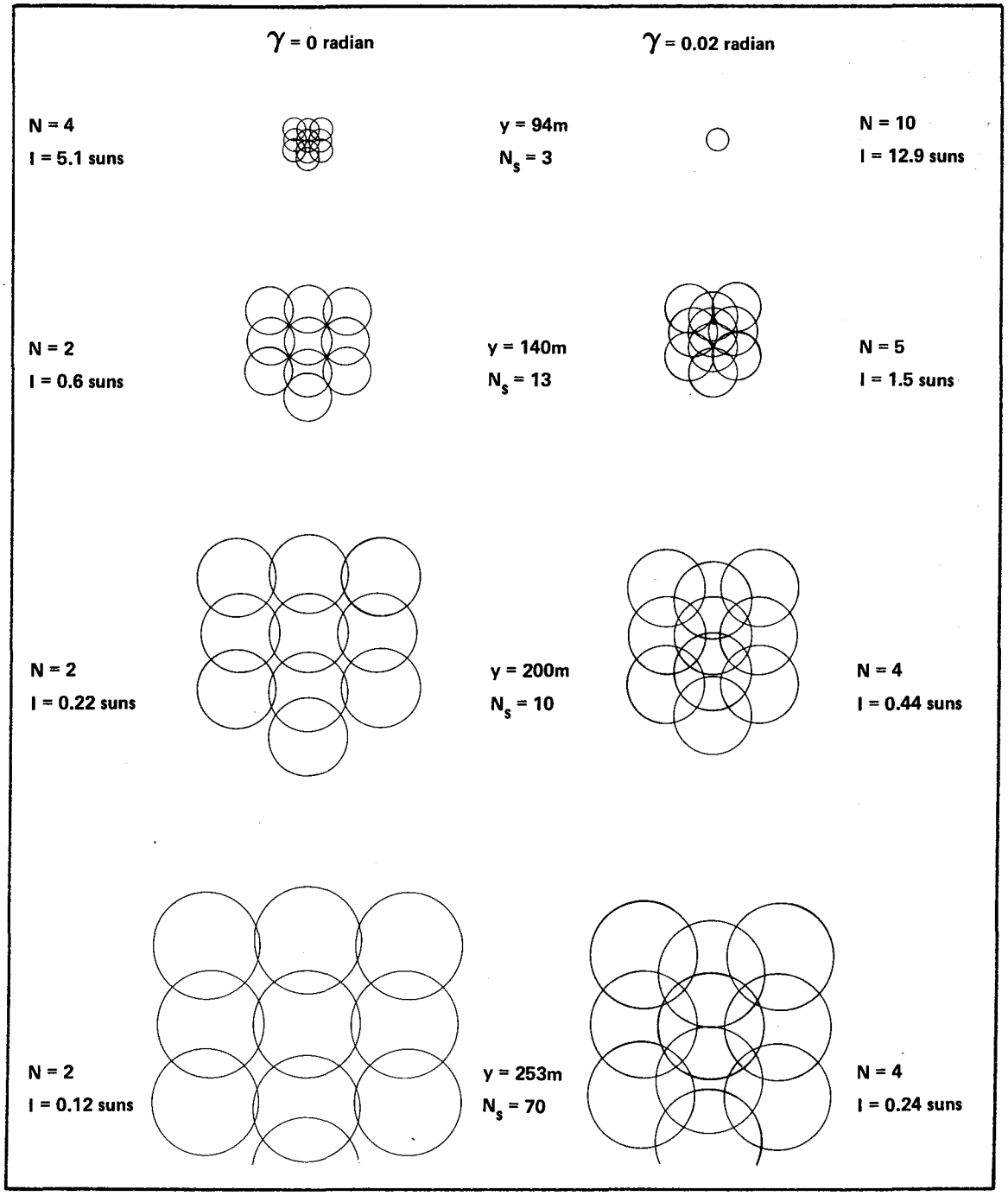

Figure 27. Progressive Expansion and Divergence of a Cluster of Ten Beams Centered 195 m North of Tower as a Function of Altitude

this example drops to one sun at about 160 m altitude with 5 beams engaged. At 140 m the composite retinal image* has already dropped below a safe diameter. Since the group in this example is limited to ten beams, the composite retinal image drops below a safe diameter at about 125 m (Figure 20). However, if the number in a group is not limited, all of the heliostats potentially coincident at a particular altitude must be considered.

Referring to Figure 25, it can be seen that at a 160 m altitude there are 13 beams which are potentially coincident. Figure 20 shows that up to about 20 coincident beams could be tolerated without reaching an unsafe retinal conditions. Thus, with the present control strategy, 160 m would be a safe altitude for beams emanating from heliostats in this part of the field.

Figure 28 shows a similar normal projection of beam centers surrounding a reference heliostat 70 m north of the tower. The nominal focal length is about 100 m. At an altitude of 150 m only 5 beams are potentially coincident. Again referring to Figure 20, up to about 10 beams could be tolerated, so this would be a safe altitude.

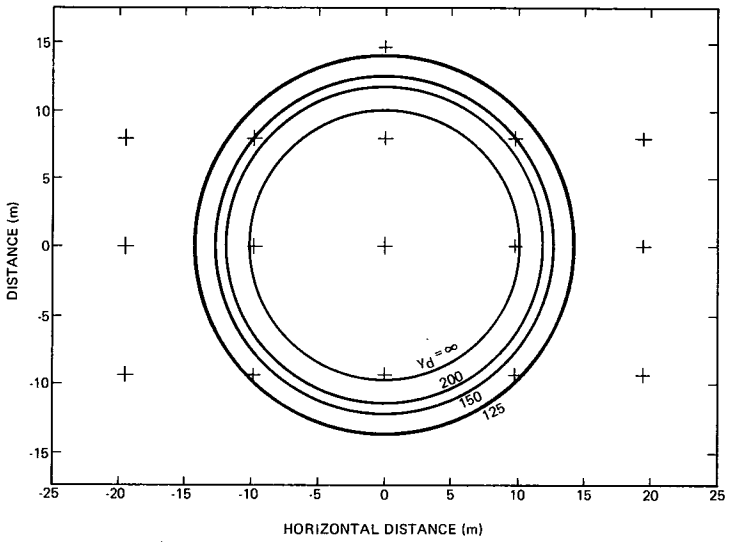

Figure 28. Normal Projection of Beams Surrounding a Reference Heliostat 70 m North of Tower

*Discrete images conservatively assumed to be coalesced to an effectively continuous circular image.

Because of the various simplifying assumptions, these analyses are only approximate. In actuality, one would expect considerable variability in flux density at any given altitude because of nonuniform flux distributions within a beam, partial engagement of beams, and systematic and random tracking errors. Consequently, further investigations are warranted using more detailed computer models, such as Mirval[6] or Helios.[7] Preliminary studies using these codes are underway and results to date are generally consistent with the findings in this report. Based upon this study, however, it appears that under normal operations the beam control strategies now incorporated will ensure that the flux density will generally not exceed one sun above an altitude of about 200 m. Slightly higher intensities may exist in small, isolated regions at higher altitudes under certain conditions. The retinal irradiance above 200 m should be well within safe levels.

Based on these analyses, a recommended aircraft exclusion zone is shown in Figure 29. The altitude of 200 m (140 m above the top of the tower) is compatible with normal FAA minimum safe altitude regulations which preclude aircraft from operating closer than 152 m (500 feet) to any structure.[12]

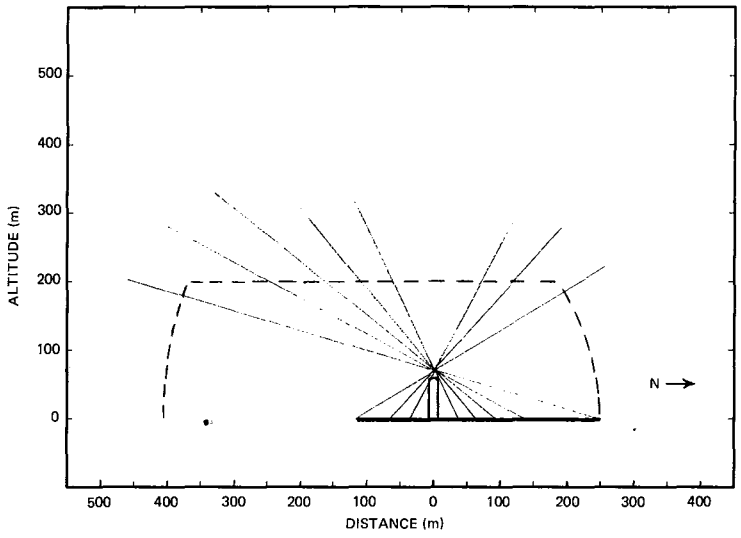

Figure 29. Recommended Aircraft Exclusion Zone Based on Safe Retinal Exposure to Reflected Light

Other Potential Hazards

Fail-Safe Shutdown

As a precaution against certain types of failures which could endanger an experiment or pose a safety hazard (such as a feedwater pump failure or loss of primary utility power), provisions are being incorporated to "trip" all of the heliostats simultaneously and quickly remove flux from the experiment. In such an event, the beams will be diverted from the receiver within 5 seconds; the heliostats will then slew to their stow position within 15 minutes.[3] In situations wherein either primary or backup power is available and the heliostat computers are operable, heliostats will move to stow in the normal manner. In certain instances involving computer breakdowns the heliostats will move directly (rather than via the "wire") to their stow positions. In such cases, discrete zones of intensities greater than one sun could momentarily extend well beyond the immediate vicinity of the test facility. Detailed analytical models are being developed to characterize the extent and duration of such momentary intensity excursions during a fail-safe shutdown. However, since such occurrences should be brief and vary rare, the likelihood of airborne personnel encountering hazardous levels should be very low.

Reflected Light From Receivers

Near the focal zone at the top of the tower, concentrated light from the heliostats and light reflected from a receiver (or other components) will be very intense. Personnel access to the tower will be prevented or stringently controlled during operations. Light reflected from receivers would also be important if levels could be high enough to constitute an eye hazard at the base of the tower, within the heliostat array, the control room, or other occupied areas.

The following simplifying assumptions can be made to conservatively bound the problem from the safety standpoint:

1. Reflective and radiative losses are diffuse. This appears to be very nearly true for the kinds of high absorptivity surfaces and other materials under consideration in the various receiver designs.

2. There are no cosine losses. This is a worst-case assumption corresponding to a viewing angle which is normal to the absorber surface.

For current receiver designs, the incident peak flux density ranges from about 0.32 MW/m^2 for the McDonnell Douglas external configuration up to about 1 MW/m^2 ($\sim$1000 suns) at the aperture of Martin Marietta's cavity receiver. The combined reflective and radiative losses are of the order of 10 percent at peak power or a maximum of about 100 suns. For far-field considerations and for diffuse radiation, the flux density decreases as the inverse square of the distance.

$$I_2 = \left(\frac{R_1}{R_2}\right)^2 I_1$$

where I_1 and I_2 represent the flux density of reflected light at distances from the receiver of R_1 and R_2, respectively.

The lowest height above ground level presently planned for receiver testing at the Solar Thermal Test Facility is about 44 meters (the 1-MW_t Martin Marietta cavity). Assuming that I = 100 suns at 1 meter from the reflecting surface, the intensity at 44 meters would be only 0.05 sun, or about 0.005 W/cm^2. The 1-meter square aperture would subtend an angle of about 1.3 degrees or a solid angle of 4.06×10^{-4} sr.

The beam radiance at 44 meters would be

$$L = \frac{0.005\ W/cm^2}{4.06 \times 10^{-4}\ sr} = 12.3\ \frac{W}{cm^2\ sr}$$

Again assuming a light-adapted eye and a corneal transmission of unity, the retinal irradiance E_r would be

$$E_r = 0.00525(12.3) = 0.065\ W/cm^2$$

This irradiance is more than two orders of magnitude below that which results from a glance at the sun, and a factor of 80 below the maximum permissible exposure (5.2 W cm^{-2}) for this source angle (from Equation (14)). Even so, the receiver would appear quite bright at this distance, and the human blink reflex and natural aversion to bright light would be operative.

Even if the concentrated flux from the mirror field were momentarily incident upon a nearby diffuse surface with much higher reflectivity, the retinal irradiance would still be at least a factor of 8 below the MPE. Thus, it appears that light from diffusely reflecting surfaces in the focal zone could not constitute a hazard to personnel at ground level or anywhere at the test

facility other than up in the tower itself. However, if the reflecting surface were specular, such as a secondary concentrator or possibly certain types of radiation shields, a more detailed analysis would be required to determine whether a potential hazard might exist.

Skin Burn

The flux intensity required to induce mild erythema (sunburn) depends strongly upon the duration of exposure. Figure 30, taken from Ham and Sliney,[11] shows this dependence. Multiple sun intensities would be sufficiently uncomfortable on the skin that evasive action would probably be taken immediately. Within a reasonably short reaction time, fairly high flux levels could be tolerated. For example, Figure 28 indicates that 20 suns could be tolerated for up to about 10 seconds with only minor effects. Because of the dependence on exposure time, however, safe criteria will need to be tailored to specific situations.

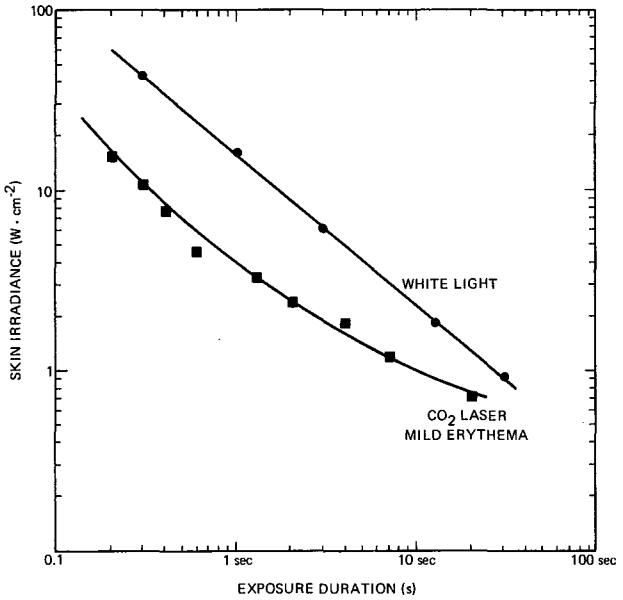

Figure 30. Pig Skin Injury Data. Lower curve is for mildest erythema for 10.6 mm IR radiation. Upper curve is white light first degree burn threshold as summarized by Davies.[11]

Fire Hazards

Experiments have shown that readily combustible materials may be ignited by radiant flux levels as low as about 20 suns.* As is evident in Figure 4, single heliostats with focal lengths less than about 125 m might be capable of igniting such materials for a short distance (20-30 m) short of or beyond their focal point. This fact may be significant for heliostats on the inner or outer perimeters of the array, since their beams could be directed at distant points at ground level without being blocked by other heliostats. Higher intensities could of course be produced by multiple coincident beams which, depending on duration of coincidence, could start fires at a considerably greater distance than a single heliostat beam.

Suggested Experiments

The validity of analytical models should be experimentally verified under key operational modes. Single beams can be readily mapped at ground level as a function of distance. For checking an array it is suggested that the flux from a group of beams at standby be characterized by means of a series of aircraft or helicopter flyovers using movie film, possibly a recording photometer, and one or more observers.

The instrumentation and personnel would be flown over the facility at selected altitudes and ranges of interest. Direct photographs of the sun using suitable neutral density filters could be used to provide a calibration reference at the beginning and end of each run. The film could then be evaluated using available densitometry and image analysis capabilities to provide both qualitative and quantitative data. This approach would simultaneously provide (1) quantitative flux measurements, (2) qualitative visual characterization, and (3) subjective human assessment, and could prove particularly helpful in evaluating distractive glint effects. The information gathered could be reviewed with a cross section of pilots and other aircraft personnel and their comments solicited.

A coordinated experimental plan should be developed by all concerned with the test facility so that tests can begin soon after installation of the Zone A heliostats.

*Simms in Reference 10 indicates the threshold of ignition to be above 1 cal $cm^{-2}s^{-1}$ (~40 suns). Recent discussions between H. Lucas, Sandia Laboratories, Livermore and N. J. Alvares, Lawrence Livermore Laboratory, indicate that ignition of dry brush may occur at about 1 cal $cm^{-2}s^{-1}$. Recent experiments by L. L. Young, Sandia Laboratories, Albuquerque, indicate that dry brush and grass found near the STTF might be ignited by peak fluxes as low as about 20 suns.

Conclusions and Recommendations

The following conclusions were drawn from this study:

1. The reflected beam from any single STTF heliostat with a focal length shorter than about 270 m constitutes a potential eye hazard that extends for a comparatively short distance on either side of its focal point. This hazard zone is generally confined to 20-30 m on either side of the focal point with the shorter focal length beams being the most hazardous.

2. Because of possible multiple beam intensities identified during initial investigations, additional beam control measures were warranted to minimize the altitudes at which overflying aircraft might encounter eye hazards.

3. The additional beam controls which were incorporated will effectively preclude intensities greater than one sun and prevent unsafe retinal irradiances at altitudes greater than about 200 meters during normal operations.

4. Momentary excursions of greater than one-sun intensity may extend to several hundred meters during certain types of fail-safe shutdown. However, these types of failures should be very rare.

5. It is believed that low-level distractive glint will not pose a hazard to aircraft personnel. Because of several subjective aspects, however, this is a difficult area to assess, and further experimental work is warranted.

6. Reflected light from diffuse surfaces located in the focal zone does not appear to present a hazard except in controlled areas near the upper part of the tower. If specular surfaces are employed, the specific configuration will need to be evaluated.

7. A potential fire hazard exists for the shorter focal length heliostats for some distance short of and beyond their focal distance if beams can impinge on combustible materials. Multiple coincident beams would, of course, increase this hazard.

8. Although the Solar Test Facility is the subject of this study, most of these findings will be similarly applicable to future central receiver pilot plants or commercial plants. Some form of beam control will undoubtedly be necessary to assure that potentially hazardous flux levels do not extend to excessive altitudes or ground distances.

Based upon this study, the following recommendations are made:

1. Continue development of detailed analytical models, and use them to more precisely determine intensity characteristics in the airspace for normal and fail-safe operational modes.

2. Verify analytical evaluations by measuring the flux produced by single and multiple beams in operational configurations. This should be done at ground level and in the airspace above the facility.

APPENDIX A--REFERENCES

1. Black and Veatch, Honeywell, Inc., Georgia Institute of Technology, "5 Megawatt Solar Thermal Test Facility, Site and Facility Requirements Definition," December 8, 1975.

2. Black and Veatch, Honeywell, Inc., Georgia Institute of Technology, "5 Megawatt Solar Thermal Test Facility, Conceptual Field Design," December 8, 1975.

3. "Solar Test Facility Heliostat Array and Control Requirements," Sandia Laboratories, Request for Quotation 03-3731, dated October 1975.

4. Black and Veatch, Honeywell, Inc., Georgia Institute of Technology, "5 Megawatt Solar Thermal Test Facility, Environmental Assessment," January 30, 1976.

5. Manual for Industrial Safety, Fire Prevention, Environmental Health, Sandia Laboratories, SC-M-70-889, Appendix B, January 2, 1975 (AFSWC Regulation 55-12, "Operations, Joint Firing Area Coordinating Committee," June 14, 1974).

6. J. D. Hankins and P. L. Leary, MIRVAL - A General Purpose, Monte Carlo Simulation, Heliostat Array and Flux Mapping Code, Sandia Laboratories, Livermore, publication of a user's manual is planned during 1977.

7. C. N. Vittitoe, F. Biggs, and R. E. Lighthill, HELIOS: A Computer Program for Modeling the Solar Test Facility, Sandia Laboratories, SAND76-0346, a user's manual to be published early in 1977.

8. D. H. Sliney, B. C. Freasier, "Evaluation of Optical Radiation Hazards," Applied Optics, Vol. 12, No. 1, January 1973.

9. R. Viskanta, J. S. Toor, "Radiant Energy Transfer in Waters," Water Resources Research, Vol. 8, No. 3, June 1972.

10. D. L. Simms, "Ignition of Cellulosic Materials by Radiation," Combustion and Flame, Vol. 4, pp. 294-300, December 1960.

11. W. M. Hamm, Jr. and D. H. Sliney, "A Study of Optical Radiation Hazards Associated With a Central Receiver Solar Thermal Power Facility," Report to be published by Black and Veatch for the Electric Power Research Institute.

12. Minimum Safe Altitudes; General, Para. 91.79, Part 91, Subchapter F, Air Traffic and General Operating Rules, Federal Aviation Regulations, Title 14 of the Code of Federal Regulations, January 1, 1973.

UNLIMITED RELEASE

INITIAL DISTRIBUTION

UC-62 (294)

U. S. Energy Research and Development Administration
Division of Headquarters Services
Library Branch, Rm. G-049
Washington, D. C. 20545

U. S. Energy Research and Development Administration (12)
Washington, D. C. 20545
Attn: H. H. Marvin
J. Braun
H. R. Blieden
G. M. Kaplan (7)
J. E. Rannels
J. P. Zingeser

U. S. Energy Research and Development Administration (5)
Albuquerque Operations Office
P. O. Box 5400
Albuquerque, New Mexico 87115
Attn: D. L. Krenz
D. K. Nowlin
J. C. Robertson
J. R. Roeder
J. A. Shurick

U. S. Energy Research and Development Administration (5)
San Francisco Operations Office
1333 Broadway
Wells Fargo Building
Oakland, California 94612
Attn: J. A. Blasy
J. T. Davis
R. W. Hughey
W. D. Nettleton
J. S. Williamson

Aerospace Corporation
P. O. Box 92957
Los Angeles, California 90045
Attn: M. Watson

Boeing Engineering and Construction
P. O. Box 3707
Seattle, Washington 98124
Attn: W. Ratcheson

Black and Veatch (3)
1500 Meadow Lake Parkway
Kansas City, Missouri 64114
Attn: J. Kintigh
M. Lippert
C. Grosskreutz

Centre National de la Recherche Scientifique
Laboratoire de L'Energie Solarie
P. P. 5 Odeillo
66120-Font-Romeu
France
Attn: C. Royere

Centre National de la Recherche Scientifique (2)
15 Quai Anatole
Paris, France, 75700
Attn: C. Etievant
M. Rodot

Electric Power Research Institute (2)
3412 Hillview Avenue
Palo Alto, California 94304
Attn: J. Cummings
J. Bigger

Federal Aviation Administration (3)
Airport District Office
P. O. Box 9253
Albuquerque, New Mexico 87119
Attn: J. R. Alexa

Georgia Institute of Technology (2)
Engineering Experiment Station
Atlanta, Georgia 30332
Attn: S. Bomar
J. D. Walton

Honeywell Systems and Research Center (3)
2600 Ridgeway Parkway
Minneapolis, Minnesota 55413
Attn: J. Powell
R. N. Schmidt
E. Zarb

Honeywell Corporation
Aerospace Division
13350 U. S. Highway 19
St. Petersburg, Florida 33733
Attn: L. P. Ball

Martin Marietta Aerospace (3)
P. O. Box 179
Denver, Colorado 80122
Attn: F. A. Blake
M. M. Hintze
T. Lebel

McDonnell Douglas Corporation (2)
5301 Bolsa Avenue
Huntington Beach, California 92647
Attn: R. Hallet
C. R. Easton

Southern California Edison
2244 Walnut Grove Avenue
Rosemead, California 91770
Attn: W. Von Kleinsmid

U. D. Army Environmental Hygiene Agency
Edgewood Arsenal, Maryland 21010
Attn: D. H. Sliney

University of Houston (2)
Department of Physics
3801 Cullen Boulevard
Houston, Texas 77004
Attn: A. F. Hildebrandt
L. Vant Hull

D. R. Parker, 3311; Attn: C. P. Skillern
L. M. Jercinovic, 3440
J. R. Doyle, 3442
A. Narath, 5000
C. N. Vittitoe, 5231
F. Biggs, 5231
J. H. Scott, 5700
G. E. Brandvold, 5710
R. P. Stromberg, 5711
J. A. Leonard, 5712
J. V. Otts, 5713 (5)
L. Young, 5713

J. Holmes, 5713
D. G. Schueler, 5719
T. B. Cook, Jr., 8000; Attn: A. N. Blackwell, 8010
C. H. DeSelm, 8200
B. F. Murphey, 8300
W. C. Scrivner, 8400
L. Gutierrez, 8100
R. C. Wayne, 8130
A. C. Skinrood, 8132
T. D. Brumleve, 8132 (40)
P. K. Lovell, 8252; Attn: H. Lucas
J. D. Hankins, 8322
P. J. Eicker, 8326
L. A. Hopkins, Jr., 9300
A. J. Clark, Jr., 9330
W. E. Caldes, 9340; Attn: J. L. Mortley, 9344
F. W. Neilson, 9350; Attn: O. J. Burchett, 9352
R. K. Petersen, 9412
C. E. Robertson, 9412
D. D. Knott, 9742
R. W. Hunnicutt, 9750
F. J. Cupps, 8265/Technical Library Processes Division, 3141
Technical Library Processes Division, 3141 (2)
Library and Security Classification Division, 8266-2 (3)